

Trinity University

Digital Commons @ Trinity

Geosciences Faculty Research

Geosciences Department

9-10-1987

Petrogenesis of Mount St. Helens Dacitic Magmas

Diane R. Smith

Trinity University, dsmith@trinity.edu

W. P. Leeman

Follow this and additional works at: https://digitalcommons.trinity.edu/geo_faculty



Part of the [Earth Sciences Commons](#)

Repository Citation

Smith, D. R., & Leeman, W. P. (1987) Petrogenesis of mount St. Helens dacitic magmas. *Journal of Geophysical Research: Solid Earth*, 92(B10), 10313-10334. <http://doi.org/10.1029/JB092iB10p10313>

This Article is brought to you for free and open access by the Geosciences Department at Digital Commons @ Trinity. It has been accepted for inclusion in Geosciences Faculty Research by an authorized administrator of Digital Commons @ Trinity. For more information, please contact jcostanz@trinity.edu.

PETROGENESIS OF MOUNT ST. HELENS DACITIC MAGMAS

Diane R. Smith

Geology Department, Trinity University, San Antonio, Texas

William P. Leeman

Department of Geology and Geophysics, Rice University, Houston, Texas

Abstract. The most frequent and voluminous eruptive products at Mount St. Helens are dacitic in composition, although a wide variety of magma types (basalt to rhyodacite) is represented. To address the petrogenesis of the dacites, we present major and trace element analyses of samples of pumice clasts and dome or flow lavas erupted during the past ~40,000 years. The dacites have similar (in some cases even lower) contents of many incompatible elements (e.g., Zr, Hf, REE, U, Be, Ta, Nb) compared with those in associated basalts and andesites, whereas Ba, Rb, K, Cs, and Sr are relatively enriched. The unusual depleted nature of the dacites and generally low bulk distribution coefficients (estimated from glass/whole - rock pairs) for numerous trace elements preclude an origin of these magmas principally by crystal fractionation of associated mafic magmas. A more plausible model for their origin involves melting of metabasaltic crustal rocks that have been enriched in Ba, Rb, Cs, and Sr by either intercalation of sediments with depleted basalt or selective metasomatic enrichment of the source region. Melting at crustal levels presumably is related to intrusion of mantle - derived basaltic magmas. Compositional diversity among the erupted dacites can be attributed to spatial or temporal heterogeneity of the magma sources or, in some specific cases, to such processes as crystal fractionation, assimilation, and magma mixing.

Introduction

During the last 40,000 years Mount St. Helens volcano (Washington state) erupted a wide range of magma types including basaltic to andesitic lavas, andesitic scoria, dacitic pumiceous tephra and pyroclastic flows, and dacitic domes and flows [e.g., Hoblitt et al., 1980; Mullineaux and Crandell, 1981]. Dacite is apparently the most frequently erupted magma type and represents the composition of all magmas erupted since May 18, 1980. We have investigated the petrology and geochemistry of all pre-1980 magma types, but here we focus on samples representing most of the documented dacite eruptions (Table 1).

The origin of dacitic magmas erupted in volcanic arcs is problematic and may involve complex interplay of several processes. Various petrogenetic models have been proposed to account for the formation of dacitic magmas including (1) closed-system crystal fractionation of basaltic or andesitic magmas [e.g., Lopez-Escobar, 1984; Berman, 1981; Reid and Cole, 1983], (2) mixing of rhyolitic and basaltic magmas [e.g., Eichelberger, 1975; Gerlach and Grove, 1982], (3) crustal contamination of mafic magma, with or without concomitant fractional crystallization [e.g., Grant et al., 1984; Francis et al., 1980; Harmon et al., 1981; Deruelle et al., 1983; Matsuhisa and

Kurasawa, 1983], (4) partial melting of the lower crust [e.g., Grant et al., 1984; Reid and Cole, 1983], and (5) formation of compositional gradients in response to convective and diffusive processes in evolving magma chambers [e.g., Smith, 1979; Hildreth, 1981].

In the present study, we describe the petrology and geochemistry of representative dacitic eruptive products and evaluate the above models for their origin at Mount St. Helens. In particular, we address possible genetic relationships among dacites, the role of basaltic and andesitic magmas as parental liquids, the involvement of crustal material in the origin of the silicic magmas, and temporal patterns in the compositions of the dacites.

Analytical Methods

The eruptive history of Mount St. Helens has been investigated through studies of detailed stratigraphic correlations, geologic mapping, carbon - 14 and tree - ring chronology, historical accounts, and remanent magnetism [Verhoogen, 1937; Lawrence, 1939, 1954; Hopson, 1971, 1972; Hyde, 1975; Crandell et al., 1975; Mullineaux et al., 1975; Crandell and Mullineaux, 1973, 1978; Hoblitt et al., 1980; Mullineaux and Crandell, 1981; Mullineaux, 1986]. Results of previous studies are summarized in Table 1. Eruptive activity during the last 40,000 years was subdivided by Mullineaux and Crandell [1981] into several eruptive periods, each lasting tens to thousands of years, separated by dormant intervals of comparable duration. Andesites were erupted during only the Castle Creek, Kalama and Goat Rocks periods, and basalts were erupted only during the Castle Creek period.

The detailed stratigraphy established by previous workers and the long-lived, though intermittent, activity at Mount St. Helens provide a unique opportunity to investigate the petrology of the eruptive units as a function of time. To this end, we sampled as many significant dacitic eruptive units as possible. To avoid possible reworked material, we collected samples of large pumice clasts from pyroclastic air-fall deposits and interior samples from domes and lava flows. There is no doubt that the samples studied are of primary magmatic origin. It was impossible to sample some key units after the 1980 eruptions; for these we obtained samples from W. G. Melson and C. A. Hopson (Goat Rocks dome, Summit dome, and Summit avalanche deposits) and from D. R. Mullineaux (Sugar Blast deposit). All dacite samples studied in detail are listed in Table 1. Thin sections were examined for all samples except those collected by Drs. Melson and Hopson that were provided to us as small chips. Analytical data for andesitic and basaltic eruptive products, shown for reference in diagrams in this paper, are from Smith [1984]; these eruptive units will be described in more detail elsewhere.

Mineral and glass analyses were determined for selected samples by electron microprobe techniques (EMP) as discussed by Smith and Leeman [1982]. Whole - rock samples selected for chemical analysis were ground in a steel rather than tungsten carbide ball mill to avoid Co

Copyright 1987 by the American Geophysical Union.

Paper number 6B5948.
0148-0227/87/006B-5948\$05.00

TABLE 1. Summary of the Eruptive History of Mount St. Helens

Eruptive Period	Age, Years B.P.	Eruptive Products	Sample Numbers	Fe-Mg Mineralogy
Ape Canyon	~40,000--35,000	Tephra layers		
		Cw	SH-8	cm, hb, bio
		Cy	SH-11	cm, hb, bio
		(Dacitic pyroclastic flows and lahars)		
Dormant interval	~15,000 years			
Cougar	20,000-18,000	Tephra layers		
		Mp	SH-14	cm, hb, hy
		Mm	SH-12	cm, hb, hy
		K	SH-13	cm, hb
		(Dacitic pyroclastic flows, domes, lavas)		
Dormant interval	~ 5000 years			
Swift Creek	13,000->8,000	(Dacitic pyroclastic flows)		
		Tephra layers		
		Sg	SH-15	cm, hb, hy
		So	SH-16	cm, hb, hy
		(Dacitic pyroclastic flows)		
		(Js)		
		Jy	SH-28	hy, hb
		Jb	SH-29	hy, hb
Dormant interval	~ 4000 years			
Smith Creek	4000-3000	Tephra layers		
		Yb	SH-19	bio, cm, hb
		Yn	SH-20	cm, hb
		Ye	SH-17	cm, hb
		(Dacitic pyroclastic flows)		
Dormant interval	~300 years			
Pine Creek	3000-2500	Tephra Layers		
		Pm	SH-21	hb, hy
		Py	SH-22	hb, hy
		(Dacitic pyroclastic flows, domes)		
Dormant interval	~300 years			
Castle Creek	~2200-1700	Tephra layers		
		(Andesitic Bo, Bh)		
		Bi	SH-24	hy, aug
		(Andesitic Bu)		
		(Basaltic to andesitic lavas and pyroclastic flows)		
Dormant interval	~600 years			
Sugar Bowl	~1150	Sugar Blast deposit	SBL-1	hy, hb (cm)
		Sugar Bowl dome	DS-63	hy, hb
		?East dome	DS-62	hy, hb
Dormant interval	~700 years			
Kalama	450-350	Tephra layers		
		Wn	SH-4	hy, hb
		We	SH-18	hy, hb
		(Dacitic pyroclastic flows; andesitic tephra layer X, lavas and pyroclastic flows)		
		Summit dome	355-1	n.d.
		Summit glowing avalanche deposits	391-1	n.d.
			1337-3	n.d.
		Lava flows	L82-43	hy, hb
			L82-46	hy, hb
			L82-54	hy, hb
			L82-58	hy, hb, aug, ol

TABLE 1. (continued)

Eruptive Period	Age, Years B.P.	Eruptive Products	Sample Numbers	Fe-Mg Mineralogy
Dormant interval Goat Rocks	~200 years 180	Tephra layer T (Andesitic lava) Goat Rocks dome	DS-41 442-1	hy, hb, aug (ol) n.d.
Dormant interval Present	~150 years	Tephra May 18, 1980 June 12, 1980 (Dacitic tephra, pyroclastic flows, domes)	MSH-1 MSH-2 6-12-80	hy, hb (aug) hy, hb (aug) hy, hb (aug)

Eruptive periods, ages, and names of eruptive units are from Mullineaux and Crandell [1981] and Hoblitt et al. [1980]. Sample numbers and ferromagnesian mineralogy for dacitic eruptive products included in this study are noted. Other Mount St. Helens eruptive products not included in this study are given in parentheses. Abbreviations: cm, cummingtonite; hb, hornblende; hy, hypersthene; bio, biotite; aug, augite; ol, olivine; and n.d., not determined.

and Ta contamination. Samples of quartz and selected internal standards (recollected BHVO-1 and BCR-1) crushed in the same manner display negligible transition metal contamination. Whole - rock samples were analyzed by inductively - coupled plasma spectrometry (ICP) for major elements and V, Cu, Be, Ba, Sr, Zr, and Zn, and by X-ray fluorescence spectrometry (XRF) for Rb, Sr, Ba, Zr, Nb, Y, Pb, V, Cr, Co, Ni, and Cu. Whole - rock and glass samples were analyzed by instrumental neutron activation analysis (INAA) for FeO, Na₂O, Sc, Cr, Co, Ni, Cs, Sr, Ba, Rb, Zn, Hf, Ta, Th, U, and the rare earth elements (REE).

Halliday et al. [1983] presented trace element data for several Mount St. Helens eruptive units, and where direct comparisons can be made, the two sets of results are in reasonable agreement. However, their Cs and Ta values are significantly higher than ours; we suspect that the latter discrepancy reflects contamination of their samples due to grinding in a tungsten carbide mill.

Petrography and Mineral Compositions

Petrography

Porphyritic clasts (white, buff, or yellow in color) of pumiceous dacite from tephra units contain plagioclase ± hypersthene ± hornblende ± augite ± cummingtonite ± biotite + iron-titanium oxide phenocrysts (> 0.3 mm) and microphenocrysts (< 0.3 mm) in highly vesicular, glassy groundmasses. Microlites (< 0.03 mm) of plagioclase ± quartz were identified in some samples by energy-dispersive microprobe analysis. The light-colored matrix glasses appear quite fresh, except for Jb and Jy tephra, in which glasses are pale yellow-orange in color and appear to be oxidized and/or hydrated. Microprobe analyses of most of the glasses show that they are rhyolitic (71 - 77 wt. % SiO₂) in composition.

Dome and flow samples are pink to light gray, nonvesicular, and porphyritic. Phenocryst minerals include plagioclase + hypersthene + amphibole ± clinopyroxene ± cummingtonite + Fe-Ti oxides. Groundmasses include very fine plagioclase, minor amounts of Fe-Ti oxides, rare quartz, and only minor amounts of glass.

Total phenocryst proportions are relatively high (Table 2) in samples representing the complete mineralogical and compositional spectrum of the dacites. Due to difficulties in point-counting highly vesicular pumice samples, weight percent modes were estimated using least - squares mass balance calculations and major element compositions of phenocrysts, glasses and whole - rocks; this method indicates phenocryst contents of 35 - 50%. Point counts of dome and lava flow samples indicate similarly high phenocryst proportions (ca. 25 - 50% by volume).

The textures of phenocrysts appear to be similar in all samples except that (1) in the pumices, plagioclase phenocrysts often are fractured and fragmented and some exhibit undulatory extinction, whereas plagioclase phenocrysts in the domes and flows are not deformed; (2) amphibole phenocryst/groundmass contacts in the lavas and domes exhibit reaction rims ("black" type of Garcia and Jacobson, [1979]) of very fine oxides, whereas amphibole phenocrysts in the pumices typically have no reaction rims; and (3) glomerophenocrysts (plagioclase ± hornblende ± hypersthene ± olivine ± Fe-Ti oxides) are more common in the domes and lavas compared with the pumices.

Mineralogy

Clinopyroxene occurs in only tephra layers Bi and T (and has been reported in some of the 1980 eruptive products; e.g., Rowley et al., 1981) as subhedral grains about 0.5 mm in diameter. Rare augite analyzed in layer T is homogeneous in composition (Wo₃₄En₅₄Fs₁₂). Minor clinopyroxene also occurs in crystal clots (+ plagioclase ± orthopyroxene ± hornblende ± olivine) in one of the Kalama lava flows (L82-58).

Biotite was found in only three units. It occurs in Yb tephra as irregularly shaped cores within hornblende phenocrysts, in Cw tephra as subhedral to euhedral microphenocrysts, and in Cy tephra as phenocrysts (up to 2 mm) rimmed by aggregates of hornblende, pyroxene, and oxides. The biotites in Cy are partially altered to chlorite and appear to be xenocrysts or phenocrysts out of equilibrium with the melt.

Minor olivine (Fo₉₉) occurs as subhedral grains within crystal clots in T tephra; it also occurs in crystal clots in

TABLE 2. Representative Modal Abundances

Sample Phenocrysts	Goat Rocks			Kalama				Sugar Bowl			Castle Creek		Smith Creek	
	Layer T	Layer We	Layer Wn	Dacite lava flows	Dacite lava flows	L82-46	L82-58	DS-63-MSH	DS-62-MSH	SH-24	DS-13-MSH	Layer Bi	Layer Yn	
	DS-41-MSH	SH-18	SH-4	L82-46	L82-58	DS-63-MSH	DS-62-MSH	SH-24	DS-13-MSH					
Plagioclase	30.4	42.2	28.9	42.2	21.6	20.2	22.2	33.0	35.4					
Olivine	trace			0.4	0.4									
Orthopyroxene	2.5	4.2	1.1	5.3	3.7	2.4	1.9	5.0						
Clinopyroxene	trace			0.8	0.8		trace	0.6						
Hornblende	5.0	2.6	5.4	0.6	0.2	0.4	trace	0.6						
Cummingtonite						trace								
Fe-Ti oxides	2.1	1.5	1.8	1.9	0.2	0.4	1.3	2.5						
Groundmass	60.0	49.5	62.8	50.0	73.1	76.6	74.6	58.9	54.7					

one of the Kalama lava flows (L82-58). In neither sample does it appear to be an equilibrium phenocryst. It has not been identified in any other dacite units.

Ilmenite and magnetite are ubiquitous in the dacites and occur as small, euhedral to subhedral inclusions in other minerals and as anhedral to subhedral microphenocrysts. Whereas Fe-Ti oxides in dacite domes are compositionally heterogeneous, those analyzed in pumice samples are relatively homogeneous (i.e., within estimated analytical errors) within as well as between individual grains. Representative analyses of oxides in numerous dacitic tephra are given in Smith and Leeman [1982] and Smith [1984].

Representative analyses of common silicate phenocrysts (plagioclase, hypersthene, hornblende, and cummingtonite) are given in Tables 3 and 4 and are displayed in Figures 1 through 3.

Intensive Parameters for Dacitic Magmas

Temperatures and oxygen fugacities were estimated for several Mount St. Helens dacites using analyses of coexisting ilmenite and magnetite and the methods of Spencer and Lindsley [1982] and Andersen and Lindsley [1985]. For W and T tephra, our estimated temperatures (820 - 965°C; Table 5) and oxygen fugacities (0.5 to 1.5 log units above the NNO buffer) are similar to those of Melson and Hopson [1981], particularly when their data are recalculated by the method used here [Stormer, 1983]. It was not possible to use this geothermometer for dome samples because the Fe-Ti oxide minerals were inhomogeneous and seem to have reequilibrated at subsolidus conditions.

More detailed estimates of physical conditions in the 1980 dacite magma chamber are provided by experimentally determined phase relations [Merzbacher and Egger, 1984; Rutherford et al., 1985] and from volcanologic models constrained by geophysical studies [Scandone and Malone, 1985]. Distributions of earthquake hypocenters for seismicity related to magma movements beneath Mount St. Helens imply the existence of a magma reservoir at depths of 7 to 9 km [Scandone and Malone, 1985]. Their estimate of water content (4.6 wt. %) in the 1980 dacite magma agrees remarkably with estimates based on the experimental studies. Rutherford et al. [1985] were able to reproduce the phase assemblage and mineral compositions in a sample of May 18 pumice at 4.6 ± 1.0 wt. % H_2O , temperature of $930 \pm 10^\circ C$, and total pressure of about 2.2 ± 0.3 kbar (corresponding to PH_2O/P_{total} of 0.6 ± 0.1 and a depth estimate of 7.2 ± 1 km).

Chemical Compositions

Major Element Compositions

Whole - rock compositions are given in Table 5. Figure 4 illustrates Harker variation diagrams for all Mount St. Helens rocks for which we have analyses, including basalts, basaltic andesites, and andesites. Here we include as dacites all rocks with SiO_2 contents within the range 62 - 70 wt. %, except as noted below.

Although layers Cy, Cw, Jb, and Jy contain typical dacite phenocryst assemblages (hornblende \pm hypersthene \pm cummingtonite \pm biotite), they have SiO_2 contents more typical of andesite (57.4 - 61.7 wt. %). Most other major element components in these samples conform to trends typical of Mount St. Helens dacites (Figure 4), except for higher Al_2O_3 (21.8 - 24.4%) and relatively low K_2O . Biotites in Cw and Cy appear altered, and Jb and Jy contain distinctive orange-brown glass; thus these samples do not appear to be fresh. La/Ce ratios for Jb and Jy

TABLE 3. Representative Hornblende Phenocryst Analyses

Unit	Jy				Jb				We				Wn				Sg			
	1	2	1	2	1	2	1	2	1	2	1	2	1	2	1	2	1*	2*	3	4
SiO ₂	42.8	44.3	44.1	47.8	44.9	45.7	40.6	42.5	44.7	45.2	41.2	42.5	44.8	45.7	46.0	46.3	42.7	44.9		
TiO ₂	2.40	2.62	2.13	1.28	1.59	2.34	2.76	3.00	1.91	1.62	2.45	2.81	1.86	1.70	0.73	0.90	2.37	0.88		
Al ₂ O ₃	11.1	9.97	11.8	7.59	9.11	9.85	14.5	10.3	8.98	7.97	13.8	10.4	8.82	8.73	9.08	8.35	13.4	8.90		
ΣFeO ³	12.5	13.7	13.4	13.1	13.7	12.2	12.6	16.1	15.6	15.9	11.9	15.7	15.2	15.3	15.3	14.6	12.5	16.5		
MnO	0.14	0.23	0.20	0.25	0.22	0.20	0.11	0.22	0.24	0.11	0.16	0.24	0.25	0.24	0.37	0.43	0.15	0.36		
MgO	14.0	13.4	13.7	14.5	13.8	15.2	12.8	11.6	13.0	12.8	14.1	12.2	13.2	12.7	12.7	13.4	12.4	13.1		
CaO	10.7	11.0	11.1	10.3	10.4	10.9	10.8	10.6	10.5	10.8	10.9	10.8	10.6	10.4	9.89	9.54	10.7	9.43		
Na ₂ O	2.30	2.08	2.22	1.45	1.82	2.00	2.22	2.18	1.79	2.22	2.44	2.13	1.82	1.76	1.89	1.57	2.65	2.07		
K ₂ O	0.26	0.29	0.30	0.18	0.25	0.23	0.26	0.30	0.26	0.26	0.26	0.25	0.30	0.28	0.21	0.21	0.40	0.20		
Σmm	96.20	97.59	98.95	96.45	95.79	98.62	96.65	96.80	96.98	96.88	97.20	97.08	96.80	96.81	96.17	95.30	97.27	96.34		
100Mg/66.4	63.1	64.4	64.4	65.9	63.8	66.6	64.2	55.9	59.4	58.6	67.2	57.7	60.4	59.3	59.1	61.4	63.6	58.1		
Mg+Mn+Fe																				

Unit	Yn				Ye				Sugar Bowl Dome				1980			
	1*	2	3*	4	5	6	1	2	3	4	5	6*		1	2	3
SiO ₂	48.5	48.7	49.3	44.0	48.2	49.3	42.7	42.9	43.2	44.9	46.6	47.1	44.3	44.5	44.8	44.4
TiO ₂	0.93	0.74	0.67	1.81	0.87	0.87	2.03	1.34	1.93	1.20	0.83	0.85	1.80	1.74	1.66	2.01
Al ₂ O ₃	8.84	8.72	7.68	12.2	9.46	9.54	13.8	12.7	13.5	10.2	9.57	9.27	10.1	10.0	9.58	10.2
ΣFeO ³	14.1	14.4	15.7	12.2	13.5	12.8	10.5	15.0	9.35	14.5	14.6	14.2	16.8	18.5	17.8	12.9
MnO	0.31	0.32	0.39	0.22	0.26	0.34	0.11	0.30	0.09	0.34	0.33	0.40	0.20	0.31	0.27	0.23
MgO	13.4	14.0	14.1	14.0	14.7	14.1	14.4	12.5	15.7	14.8	14.1	14.4	12.5	11.6	12.3	12.3
CaO	9.34	9.21	8.57	10.3	9.70	9.59	10.7	9.87	10.8	9.25	9.79	9.31	10.3	10.0	10.4	10.8
Na ₂ O	1.14	1.35	1.17	1.75	1.20	1.36	2.05	1.65	2.09	1.72	1.23	1.30	2.54	2.58	2.47	2.13
K ₂ O	0.22	0.22	0.20	0.23	0.15	0.23	0.27	0.24	0.24	0.19	0.18	0.15	0.39	0.32	0.31	0.35
Σmm	96.78	97.66	97.78	96.71	98.04	98.13	96.56	96.50	96.90	97.10	97.23	96.98	98.93	99.55	99.59	95.32
100Mg/62.3	62.9	61.0	61.0	66.6	65.6	65.7	70.7	59.3	74.8	64.0	62.7	63.7	56.7	52.2	54.8	62.5
Mg+Mn+Fe																

Hornblende analyzed in Sugar Bowl Dome is fairly homogeneous in composition, in contrast to individual hornblende grains within single pumice clasts from layers We, Wn, Ye, and Yn that exhibit a large range in composition [Smith and Leeman, 1982]. The majority of grains in these and other tephra have fairly uniform Ca:Mg:Fe ratios (cf. Figure 3).

* Rims around grains of cummingtonite.

† From Scheidegger et al. [1982].

TABLE 4. Representative Cummingtonite Phenocryst Analyses

Unit	Sg			Ye				
	1	2	3*	1	2	3	4	5
SiO ₂	53.9	54.3	55.0	53.9	54.5	53.8	54.8	55.2
TiO ₂	0.23	0.21	0.19	0.21	0.21	0.18	0.35	0.15
Al ₂ O ₃	2.74	2.02	3.54	2.71	2.13	3.13	1.73	2.24
ΣFeO	19.2	21.3	19.3	19.9	20.5	19.0	20.1	18.4
MnO	0.69	0.60	0.70	0.70	0.74	0.67	0.70	0.70
MgO	19.6	17.5	18.2	18.2	17.7	19.4	17.5	20.1
CaO	1.23	1.39	1.47	1.87	1.94	1.48	2.74	1.33
Na ₂ O	0.74	0.07	0.50	0.16	0.17	0.32	0.12	0.13
Sum	98.33	97.39	98.90	97.65	97.89	97.98	98.04	98.24
100Mg/ Mg+Mn+Fe	63.7	58.7	61.8	61.1	59.9	63.7	65.2	60.0

Some cummingtonites are completely to partially rimmed by green hornblende; both rimmed and unrimmed cummingtonites are compositionally homogeneous, except for a few unrimmed grains that exhibit slight reverse zoning.

* Analysis of a grain rimmed by hornblende.

(0.63 - 0.68) are slightly higher than the range for other Mount St. Helens dacites (0.43 - 0.50). Ludden and Thompson [1979] noted that the light rare earth elements (LREE), particularly Ce, may be mobilized during low-temperature weathering processes. Halliday et al. [1983] discussed similar compositional anomalies (notably in their sample of So tephra) that they tentatively attributed to an ill-defined vapor phase fractionation/volatilization process. It is assumed that these anomalous samples are altered and not strictly representative of magmatic compositions; subsequently, we place greater petrogenetic emphasis on the fresher dacites.

Samples of the Sugar Blast deposit and the Sugar Bowl and East dome lavas are distinctive from other dacites with respect to major and trace element contents. Although Mullineaux and Crandell [1981] note the uncertain timing of the East dome eruption, the similarity of the three samples studied suggests that all of these rhyodacite deposits formed during the same eruptive period. In further discussions, we assume a Sugar Bowl eruptive period age (~1150 years B.P.) for the East dome.

Overall, the Mount St. Helens eruptive products follow Harker variation trends characteristic of calcalkaline

volcanic centers [Gill, 1981]. Al₂O₃ shows little variation (excluding the "altered" dacites) with increasing silica, but TiO₂, FeO, MgO, and CaO decrease, whereas K₂O and Na₂O increase. All but one (Cy; altered?) of the analyzed dacites conform to a calcalkaline trend in Figure 5. For

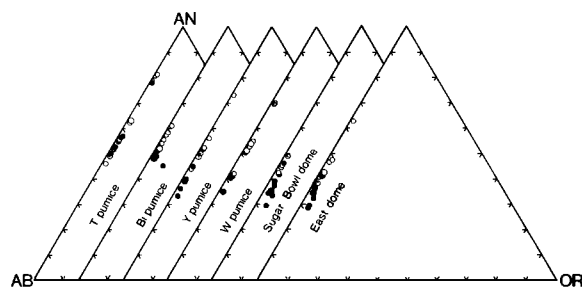


Fig. 1. Analyses of plagioclase phenocryst cores (solid circles) and phenocryst rims, microphenocrysts, and groundmass grains (solid circles) occurring in selected Mount St. Helens dacites. Oscillatory and reverse zoning are observed, but phenocryst cores are generally more calcic than phenocryst rims and groundmass grains.

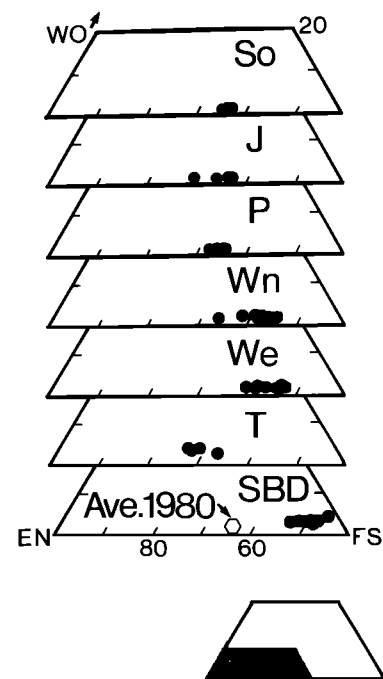


Fig. 2. WO-EN-FS variations in hypersthene phenocrysts in selected Mount St. Helens dacites. Most individual phenocrysts are nearly homogeneous or normally zoned, but some phenocrysts (e.g., in pumice layers We, Wn, and Sugar Bowl dome) exhibit small Mg enrichments toward the rim. Due to overlapping compositions, data for layers Jy and Jb and layers Pm and Py are plotted together (J and P, respectively). Average hypersthene composition for May 18, 1980, pumice taken from Scheidegger et al. [1982].

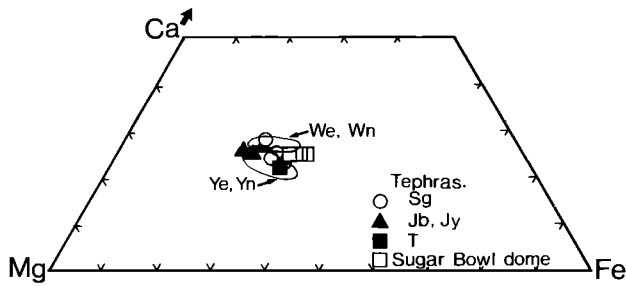


Fig. 3. Ca-Mg-Fe variations in hornblende in Mount St. Helens dacites. Data for nearly coeval tephra (e.g., We and Wn) are plotted together, as these hornblendes are indistinguishable on this diagram.

comparison, published analyses [Lipman et al., 1981; Cashman and Taggart, 1983] of dacites erupted since 1980 are included in Figure 5; their compositional range is relatively limited compared with that for all Mount St. Helens dacites.

Trace Element Abundances

Trace element compositions of whole - rocks and glass separates are given in Tables 5 and 6, respectively. For the entire eruptive suite, ranges for many trace element abundances overlap somewhat among the basalts, basaltic andesites, and dacites. With increasing SiO_2 contents, however, (1) abundances of Sc, V, Cr, Co, Ni, Sr, Zn, Cu, Ta, Nb, heavy rare earth elements (HREE), and Y generally decrease, (2) abundances of Cs, Rb, Ba, and Th increase, and (3) the LREE, Zr, Hf, Be, and U appear to be nearly constant or slightly decrease.

Temporal Trends

Excluding presumably "altered" samples, most dacitic magmas erupted early (prior to 2200 years B.P.) in the history of Mount St. Helens have fairly similar compositions, both within and between eruptive periods (Figures 6a through 6c). The exception is tephra layer K (erupted late in the Cougar eruptive period), which is slightly more evolved than other pre-Castle Creek dacites.

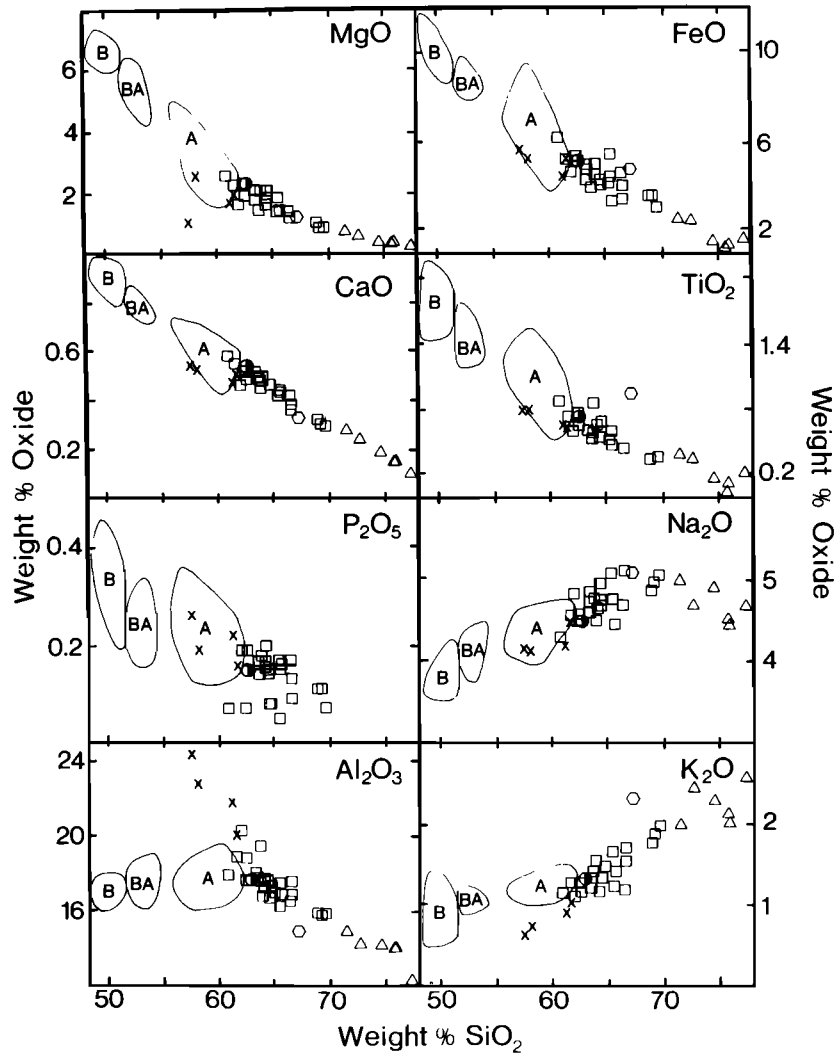


Fig. 4. Harker variation diagrams for Mount St. Helens eruptive products. Symbols as follows: open squares, dacites (whole rock); open triangles, glass matrices of dacite pumices; crosses, "altered" dacites; and open hexagon, glass matrix of andesitic scoria. Fields are shown for Mount St. Helens basalts (B), basaltic andesites (BA), and andesites (A). Half - solid circle represents average composition of 1980 - 1982 eruptive products (cf. Table 5). Data for fields and points not given in Table 5 can be found in the work by Smith [1984].

TABLE 5. Whole Rock Major and Trace Element Analyses

	Ape Canyon		Cougar			Swift Creek			
	Cw SH-8	Cy SH-11	Mp SH-14	Mm SH-12	K SH-13	Sg SH-15	So SH-16	Jy SH-28	Jb SH-29
<u>Major Elements, %</u>									
SiO ₂	61.13	57.44	62.47	61.66	66.53	63.67	61.93	61.59	58.10
TiO ₂	0.67	0.80	0.67	0.71	0.47	0.55	0.60	0.64	0.80
Al ₂ O ₃	21.79	24.37	18.85	18.86	17.63	19.47	20.24	20.11	22.73
FeO	4.58	5.72	5.25	5.40	3.51	4.04	4.76	4.67	5.40
MnO	0.07	0.09	0.07	0.08	0.06	0.07	0.07	0.07	0.07
MgO	1.67	1.01	1.95	2.25	1.20	1.44	1.63	1.92	2.51
CaO	4.69	5.40	4.79	5.28	3.64	4.49	4.57	4.99	5.22
Na ₂ O	4.20	4.19	4.40	4.48	4.68	4.45	4.40	4.67	4.14
K ₂ O	0.90	0.65	1.11	1.04	1.48	1.21	1.13	1.11	0.75
P ₂ O ₅	0.22	0.26	0.19	0.15	0.09	0.18	0.19	0.15	0.19
<u>Trace Elements, ppm</u>									
La	10.1	8.6	9.7	9.0	11.7	11.2	9.1	8.2	7.1
Ce	20.2	20.2	21.8	20.5	-	24.8	19.8	12.0	11.3
Sm	3.03	3.49	2.75	2.59	2.10	2.70	2.40	2.19	2.67
Eu	0.90	1.06	0.84	0.89	0.82	0.88	0.84	0.75	0.84
Tb	0.42	0.44	0.40	0.35	0.28	0.38	0.34	0.31	0.38
Yb	0.99	1.11	1.04	0.93	0.82	1.00	0.93	0.98	1.02
Lu	0.15	0.18	0.17	0.15	0.13	0.16	0.16	0.15	0.14
Y	-	-	12.0	-	8.3	9.9	9.5	-	-
Sc	6.2	8.5	7.9	9.2	5.2	6.2	7.2	8.9	9.9
V	69	87	71	84	39	56	65	86	103
Co	7.6	10.5	10.5	12.2	6.0	7.3	8.0	10.9	11.6
Cs	0.99	0.57	1.21	1.02	1.97	1.48	1.16	1.47	1.65
Rb	20	9	28	23	38	29	26	30	36
Sr	493	571	483	574	481	511	506	503	478
Ba	210	-	277	293	395	298	291	276	187
Zr	-	-	135	-	151	122	149	99	121
Hf	3.5	4.2	3.3	3.2	3.8	3.4	3.6	3.2	3.5
Ta	0.48	0.59	0.41	0.42	0.53	0.43	0.44	0.32	0.32
Nb	-	-	-	-	-	-	-	-	-
Th	2.72	3.37	2.48	2.30	3.61	2.64	2.77	2.48	2.70
Zn	62	62	55	57	51	57	60	57	62
Cu	12	10	12	10	5	6	8	14	14
Be	1.9	1.8	0.9	1.1	1.7	1.5	1.5	1.3	1.3
U	0.7	0.7	0.6	0.5	0.7	0.6	0.7	0.8	0.7
<u>Temperatures, °C</u>									
T, °C*	-	-	940	945	845	900	870	-	-
T, °C†	-	-	870	870	825	845	840	-	-

The most voluminous eruptions of mafic magma types (basalt to andesite) occurred during Castle Creek time (2200 - 1700 years B.P.) and were accompanied by only minor eruptions of dacite (e.g., tephra layer Bi). The subsequent Sugar Bowl rhyodacites are the most evolved silicic magmas yet erupted from Mount St. Helens. During both the Kalama (450 - 350 years B.P.) and Goat Rocks (180 years B.P.) periods the erupted dacites are more diverse. The Kalama dacites span nearly the whole compositional range exhibited by all other Mount St. Helens dacites, whereas the range for dacites from the Goat Rocks eruptive period is relatively small.

Ba/La, Rb/Cs, Hf/Ta, and Ta/Yb ratios are similar in all Mount St. Helens dacites (excluding the "altered"

samples), with the exception of dacites erupted during the Kalama period (Figures 6d through 6i). The other ratios illustrated (Th/Cs, Ba/Cs) exhibit more variation, both within and between eruptive periods. The Kalama dacites are notable in that they display a wide range in all the ratios plotted.

Glass/Whole - Rock Elemental Ratios

Glass/whole - rock ratios for numerous elements (Figure 7) are useful in evaluating the effects of differentiation (e.g., crystal fractionation) on the abundances of trace elements in residual liquids (matrix glasses). The glasses in all but one sample are rhyolitic,

TABLE 5. (continued)

	Smith Creek			Pine Creek		Castle Creek	Sugar Bowl		
	Yb SH-19	Yn SH-20	Ye SH-17	Pm SH-21	Fy SH-22	Bi SH-24	Sug.Blast SBL-1	Sug.Dome DS-63	EastDome DS-62
<u>Major Elements, %</u>									
SiO ₂	64.47	65.43	66.48	63.32	64.18	64.10	69.57	69.20	69.02
TiO ₂	0.56	0.48	0.47	0.62	0.60	0.67	0.37	0.37	0.35
Al ₂ O ₃	17.69	17.54	16.57	18.08	17.77	17.36	15.93	15.89	15.90
FeO	4.46	4.47	4.69	4.85	4.66	5.08	3.11	3.62	3.67
MnO	0.07	0.07	0.07	0.08	0.07	0.07	0.07	0.06	0.03
MgO	1.59	1.40	1.41	1.93	1.84	1.73	0.85	0.83	0.99
CaO	4.66	4.39	4.16	5.07	4.79	4.52	2.99	3.05	3.22
Na ₂ O	4.55	4.59	4.69	4.61	4.64	4.68	5.05	4.97	4.86
K ₂ O	1.21	1.34	1.20	1.21	1.18	1.54	1.97	1.86	1.76
P ₂ O ₅	0.14	0.15	0.17	0.16	0.20	0.17	0.07	0.11	0.11
<u>Trace Elements, ppm</u>									
La	10.7	10.6	10.8	10.2	11.8	11.9	15.2	16.0	15.1
Ce	-	-	25.3	22.3	24.8	24.8	33.2	34.8	31.2
Sm	2.49	2.32	2.62	2.68	2.80	2.62	3.41	3.17	3.00
Eu	0.85	0.82	0.86	0.85	0.91	0.85	0.88	0.86	0.87
Tb	0.35	0.22	0.35	0.37	0.38	0.40	0.50	0.40	0.39
Yb	0.82	0.73	0.83	0.89	0.95	1.33	1.37	1.29	1.24
Lu	0.12	0.12	0.13	0.15	0.15	0.19	0.21	0.20	0.19
Y	9.2	9.5	11.0	11.7	13.0	-	-	14.5	14.4
Sc	5.6	5.5	5.8	8.1	7.6	8.3	4.3	4.8	5.3
V	54	50	48	78	74	69	20	24	30
Co	8.5	7.7	8.1	10.9	10.2	10.4	4.6	5.1	5.7
Cs	1.32	1.21	1.23	1.23	1.23	2.06	2.14	2.42	2.14
Rb	30	29	30	30	31	39	52	54	50
Sr	521	508	502	515	510	427	351	365	369
Ba	287	334	380	321	356	351	449	430	462
Zr	118	126	122	124	135	130	161	173	167
Hf	3.1	2.9	3.1	2.8	3.1	3.3	3.8	4.3	4.1
Ta	-	0.36	0.42	0.38	0.47	0.43	0.55	0.62	0.57
Nb	-	-	6.9	7.0	9.3	-	-	8.3	8.5
Th	2.06	2.02	2.20	1.95	2.33	2.76	3.60	3.65	3.40
Zn	61	66	59	62	59	54	-	55	56
Cu	11	-	13	16	18	26	-	14	14
Be	1.1	1.3	1.4	1.3	1.5	1.5	-	1.8	1.8
U	0.5	0.5	0.6	0.5	0.6	0.7	-	1.1	1.0
<u>Temperatures, °C</u>									
T, °C*	-	845	860	905	945	940	-	-	-
T, °C†	-	820	830	855	880	905	-	-	-

the exception (shown in Figure 7c) being a Kalama period andesitic scoria from tephra layer X. Dacitic glass in this scoria contains phenocrysts of orthopyroxene + clinopyroxene + plagioclase + Fe-Ti oxides. Using estimated proportions of glass (i.e., residual liquid; Table 2), the empirical glass/whole - rock enrichment factors (Figure 7), and the equation for Rayleigh fractionation, we calculated apparent bulk distribution coefficients (D values) for a variety of elements (Table 7). Several features of the apparent D values are notable:

1. Relatively large D's (1.3 - 2.2) for Sr are consistent with the incorporation of this element by plagioclase [e.g., Philpotts and Schnetzler, 1970], which is the dominant phenocryst phase.

2. Although generally considered to be incompatible, Ta exhibits relatively large D values approaching unity that suggest it is significantly partitioned into some phase(s). High Ta distribution coefficients (18 - 106) have been empirically determined for ilmenite coexisting with rhyolitic liquid [Mahood and Hildreth, 1983; Nash and Crecraft, 1985]. Pearce and Norry [1979] inferred high Nb partition coefficients for hornblende and magnetite; presumably Ta would exhibit similar geochemical behavior.

3. D values for Hf and Zr are relatively high (~0.25 to 0.60) but may be explained by the incorporation of these elements in hornblende. Pearce and Norry [1979] estimated Zr distribution coefficients ranging from 1.4 to

TABLE 5. (continued)

Kalama									
	Wn	We	Sum.Dome	Avalanches		Lava Flows			
	SH-4	SH-18	355-1	391-1	1337-3	L82-43	L82-46	L82-54	L82-58
<u>Major Elements, %</u>									
SiO ₂	66.54	65.32	64.00	65.43	60.80	64.56	64.74	63.88	64.52
TiO ₂	0.46	0.52	0.64	0.61	0.87	0.61	0.61	0.86	0.69
Al ₂ O ₃	16.97	17.29	17.14	16.26	17.90	17.24	17.32	16.86	16.74
FeO	4.07	4.25	4.37	5.52	6.29	4.32	4.19	5.07	4.44
MnO	0.07	0.07	0.07	0.07	0.09	0.08	0.08	0.09	0.08
MgO	1.16	1.38	2.09	1.83	2.59	1.90	1.90	1.68	2.12
CaO	3.87	4.16	4.95	4.46	5.84	4.64	4.65	4.68	4.56
Na ₂ O	5.12	5.10	4.50	4.48	4.29	4.68	4.70	4.78	4.75
K ₂ O	1.55	1.67	1.49	1.23	1.16	1.47	1.47	1.55	1.50
P ₂ O ₅	0.13	0.17	0.15	0.05	0.07	0.08	0.08	0.18	0.15
<u>Trace Elements, ppm</u>									
La	12.6	12.3	8.0	7.3	7.6	9.3	-	14.9	13.5
Ce	26.7	26.5	16.8	16.1	16.6	19.0	-	33.0	30.0
Sm	2.49	2.62	1.70	1.43	1.92	2.01	-	3.83	3.12
Eu	0.84	0.87	0.76	0.83	0.92	0.81	-	1.11	0.97
Tb	0.40	0.39	0.25	0.26	0.28	0.29	-	0.60	0.45
Yb	1.16	1.15	0.91	1.01	1.24	1.11	-	1.66	1.30
Lu	0.17	0.17	0.14	0.16	0.21	0.18	-	0.25	0.20
Y	-	13.5	-	-	-	10.0	9.6	9.8	14.0
Sc	5.8	6.4	9.6	9.6	11.7	9.1	9.3	10.8	9.3
V	40	49	63	-	100	69	56	-	58
Co	7.2	8.5	12.6	11.8	16.4	12.1	-	12.6	12.1
Cs	1.84	1.76	1.12	1.94	0.96	1.11	-	1.71	1.44
Rb	43	40	34	38	32	37	37	47	37
Sr	404	448	441	-	567	446	451	465	450
Ba	397	372	310	340	290	343	369	-	367
Zr	126	142	120	130	130	137	135	177	148
Hf	3.5	3.5	3.2	3.3	3.4	3.5	-	4.0	3.7
Ta	0.46	0.47	0.36	0.34	0.44	0.34	-	0.47	0.55
Nb	-	7.5	-	-	-	6.7	8.7	9.8	10.0
Th	2.77	2.64	2.16	2.31	2.13	2.80	-	3.20	2.80
Zn	54	54	55	-	64	50	49	74	54
Cu	14	12	35	-	26	26	16	47	19
Be	1.5	1.7	0.8	-	1.2	-	-	-	-
U	0.6	0.5	0.7	-	0.7	-	-	-	-
<u>Temperatures, °C</u>									
T °C*	845	850	-	-	-	-	-	-	-
T °C†	840	840	-	-	-	-	-	-	-

4.0 for hornblende in intermediate to silicic magmas; Hf may exhibit similar behavior. The anomalously high D values (~1.0 - 1.1) for Hf in layers Yn and Ye can be explained by the presence of cummingtonite in addition to hornblende; Rose et al. [1979] have reported high Hf distribution coefficients (>1) for cummingtonite.

4. Excluding Eu, estimated D's for the REE are moderate and range from ~0.20 to 0.80. Slightly higher D values for the HREE versus LREE in layers Ye, T, and Wn are consistent with fractionation of amphibole, which preferentially incorporates the HREE [e.g., Arth and Barker, 1976]. Estimated D values for Eu are close to or

greater than 1.0 and are consistent with incorporation of Eu in plagioclase [e.g., Sun et al., 1974; Drake and Weill, 1975].

5. Estimated D's for Ba, Rb, Th, and Cs are larger than expected (e.g.; D^{Ba} , $D^{Cs} \approx 0.50 - 0.70$), as these elements are not known to be incorporated to any significant degree by the observed phenocryst phases. These elements are not enriched in the glasses commensurate with the estimated degree of crystallization. It seems unlikely that such large D's for these elements could be attributed solely to analytical errors or inaccurate estimates of phenocryst/glass

TABLE 5. (continued)

	Goat Rocks		Present					Estimated Errors, % of Amount Present§
	T DS-41	GRDome 442-1	May 18, 1980 MSH-1	May 18, 1980 MSH-2	June 12, 1980 6-12-80	Average‡	1σ	
<u>Major Elements, %</u>								
SiO ₂	63.46	62.43	61.90	62.00	63.60	62.60	0.50	1(ICP)
TiO ₂	0.59	0.77	0.70	0.66	0.61	0.68	0.03	3(ICP)
Al ₂ O ₃	17.74	17.73	17.30	17.50	17.65	17.80	0.20	1(ICP)
FeO	4.99	5.46	4.65	4.43	4.78	5.14	0.15	3(ICP)
MnO	0.09	0.09	0.07	0.07	0.07	0.076	0.005	4(ICP)
MgO	1.78	2.32	1.94	1.80	1.94	2.22	0.12	4(ICP)
CaO	5.00	5.21	5.20	5.12	5.01	5.35	0.14	3(ICP)
Na ₂ O	4.85	4.58	4.82	4.93	4.72	4.48	0.08	3(ICP)
K ₂ O	1.27	1.27	1.39	1.31	1.41	1.29	0.05	3(ICP)
P ₂ O ₅	0.16	0.07	0.15	0.16	0.14	0.15	0.01	3(ICP)
<u>Trace Elements, ppm</u>								
La	11.2	8.3	13.1	13.6	11.0	-	-	3(INAA)
Ce	23.3	18.1	28.6	28.4	23.9	-	-	4(INAA)
Sm	2.17	1.83	3.01	3.11	2.36	-	-	4(INAA)
Eu	0.85	0.87	0.93	0.92	0.80	-	-	3(INAA)
Tb	0.36	0.27	0.38	0.36	0.35	-	-	7(INAA)
Yb	1.19	1.09	1.18	1.22	0.97	-	-	5(INAA)
Lu	0.18	0.16	0.20	0.20	0.16	-	-	4(INAA)
Y	13.1	-	-	-	-	-	-	5(XRF/ICP)
Sc	8.2	11.2	9.3	8.9	8.6	-	-	3(INAA)
V	71	89	80	74	-	-	-	7(ICP)
Co	11.7	13.8	11.9	11.1	11.1	-	-	4(INAA)
Cs	1.17	1.50	1.14	1.27	1.29	-	-	6(INAA)
Rb	31	37	29	33	26	-	-	3/10(XRF/INAA)
Sr	470	507	452	463	463	-	-	5(XRF/ICP)
Ba	341	320	328	320	296	-	-	7(XRF/ICP)
Zr	130	110	122	123	111	-	-	5(XRF/ICP)
Hf	3.2	3.4	3.2	3.5	3.0	-	-	5(INAA)
Ta	0.42	0.40	0.52	0.52	0.34	-	-	7(INAA)
Nb	6.7	-	-	-	-	-	-	5(XRF)
Th	2.16	2.18	2.38	2.40	2.23	-	-	7(INAA)
Zn	63	55	53	55	-	-	-	8(XRF/ICP)
Cu	25	28	44	40	-	-	-	15(XRF/ICP)
Be	1.5	1.1	1.3	0.9	-	-	-	10(ICP)
U	0.7	0.9	0.8	1.0	-	-	-	15(INAA)
<u>Temperatures, °C</u>								
T, °C*	965	-	-	-	-	-	-	-
T, °C†	915	-	-	-	-	-	-	-

All samples except L82-43, -46, -54, and -58 were analyzed by ICP (Barringer Resources), INAA (D. Smith and W. Leeman, Oregon State University and NASA-JSC), and XRF (W. Leeman, Open University). The L82-series samples were analyzed by G. Fitton (XRF, major and trace elements, University of Edinburgh) and M. Norman (INAA, NASA-JSC).

Analyses are listed by eruptive period, eruptive unit, and sample number.

* Temperature calculated using the equations of Spencer and Lindsley [1982].

† Temperature calculated using the equations of Anderson and Lindsley [1985].

‡ The average composition for the present eruptive period dacites is from Cashman and Taggart [1983].

§ The last column lists estimated analytical errors (given in percent of amount present) and the technique(s) by which an element was determined (in parentheses). Where an element was determined by more than one technique the value given is either (1) a single value obtained by the technique which yielded the highest quality data (as judged by analyses of standard rocks BCR-1, AGV-1, GSP-1, and BHVO-1, or (2) an average of values obtained by multiple techniques where analytical precision and accuracy are comparable.

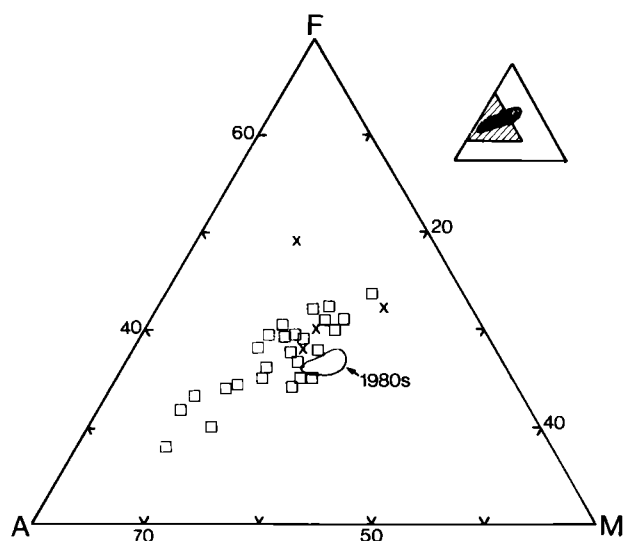


Fig. 5. AFM diagram for Mount St. Helens dacites. Symbols as in Figure 4. Inset shows range for all Mount St. Helens eruptive products [Smith, 1984]. Outlined field for 1980 - 1982 eruptive products [Cashman and Taggart, 1983; Lipman et al., 1981].

proportions. It is possible that selective loss of these elements from the liquids (matrix glasses) occurred via volatile transfer or some other process. Ba, Rb, and Cs have low ionic potentials and are expected to be relatively mobile in an aqueous fluid (e.g., vapor) phase [Pearce, 1983].

To evaluate possible effects of volatile transfer processes in depleting residual liquids (matrix glasses) in Ba, Rb, Th, and Cs, we examined coeval pumice and dome deposits of the Goat Rocks and Kalama periods. The pumices (layers T, We, and Wn) in each period were erupted early, presumably by explosive ejection of water-saturated magmas. The domes (Goat Rocks and Summit domes) formed later by quieter extrusion of less hydrous magmas. Tapping of a progressively water-

depleted magma chamber is fairly well documented for the 1980 eruptions and is supported by the progressive decrease in the explosivity of the eruptions [Scandone and Malone, 1985] and decreases in estimated water contents of early and later erupted products [Melson, 1983; Merzbacher and Egger, 1984].

If coeval pumice and dome magmas were derived from zoned magma chambers, and if compositional zonation resulted from fractionation and/or volatile transfer processes, we would expect hygromagmatic elements to be enriched in earlier erupted magmas (from H₂O-enriched upper parts of the chamber) to a comparable or greater degree relative to other incompatible elements (e.g., REE). Pumice:dome ratios for eruptive products of the Goat Rocks and Kalama periods (Figure 8a) show the opposite effect: (1) in the Goat Rocks products, Ba, Rb, Th, and Cs show no enrichment, whereas the REE are slightly enriched; and (2) in the Kalama products, the hygromagmatic elements are not enriched to the degree expected. Because corresponding bulk D values are expected to be very small ($\ll 1$), these elements theoretically should display greater enrichments than the REE, for example. The observed fractionation patterns suggest that Ba, Rb, Cs, and Th are relatively depleted in the early erupted magmas. Rutherford et al. [1985] and Melson [1983] showed that glass inclusions in phenocrysts in 1980 pumices have higher inferred water contents than corresponding matrix glasses. These observations suggest that explosive eruptions resulted in differential loss of volatiles from the host liquids (matrix glass). Thus escape of volatiles during explosive eruptions may have mobilized the hygromagmatic elements, causing their apparent relative depletion in residual silicate liquids. Of course, observed incompatible element fractionation patterns and compositions of the dacites may be primary magmatic characteristics.

Petrogenesis of Mount St. Helens Dacites

As noted earlier, dacitic magmas may originate through complex operations of several petrogenetic processes [cf. Green, 1980]. Here, we rely primarily on trace element abundances in Mount St. Helens eruptive products to evaluate some plausible hypotheses for the origin of these magmas.

TABLE 6. INAA Trace Element Analyses of Selected Mount St. Helens Samples

	Unit						
	T	We	Wn	Bi	X	Yn	Ye
La	15.7	17.4	17.2	17.1	22.1	15.5	15.8
Ce	33.1	38.1	36.1	38.3	50.0	33.9	35.2
Sm	3.31	3.96	3.54	4.34	5.54	3.00	3.23
Eu	0.81	0.71	0.74	0.96	1.56	0.72	0.74
Tb	0.44	0.54	0.44	0.64	0.76	0.31	0.34
Yb	1.59	1.60	1.41	2.06	2.11	0.90	0.87
Lu	0.22	0.25	0.20	0.28	0.31	0.12	0.13
Sc	5.2	4.9	3.4	6.7	13.0	1.8	2.6
Co	4.3	2.6	2.0		5.8	1.7	2.3
Cs	1.63	2.29	2.10	2.50	1.27	1.64	1.76
Rb	50	63	56	56	46	47	47
Sr	290	195	263	232	420	264	280
Ba	420	525	460	542	452	449	445
Zr	183	188	151		256	160	137
Hf	4.2	4.9	4.4	4.9	5.0	2.7	3.1
Ta	0.44	0.48	0.46	0.48	1.19	0.44	0.46
Th	3.07	4.26	3.99	3.73	3.45		3.56

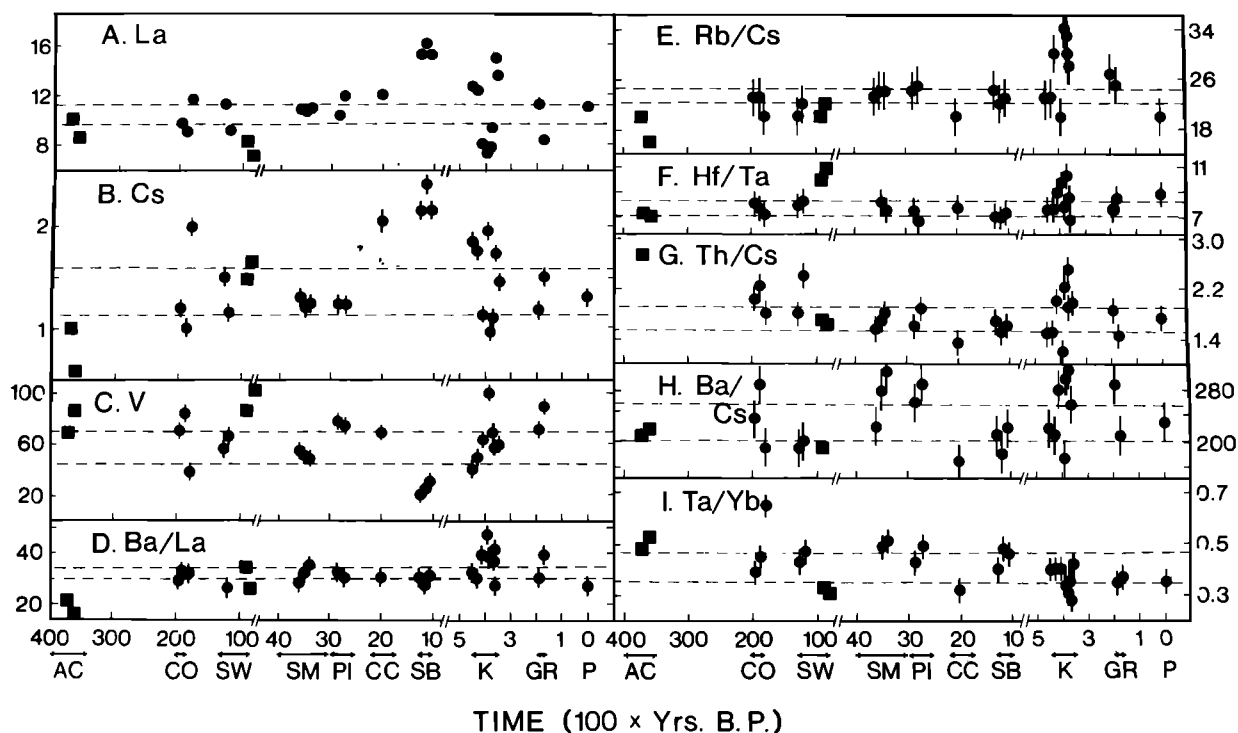


Fig. 6. (a - c) Selected trace element abundances (in parts per million) and (d - i) ratios in Mount St. Helens dacites and rhyodacites plotted as a function of approximate time of eruption. Open circles represent "altered" dacites. Bars represent estimated analytical errors; in Figure 6a the symbols encompass estimated errors. The mean and one standard deviation (1σ) were calculated for each ratio or concentration (excluding altered dacites). Samples with values outside the mean $\pm 1\sigma$ were dropped; dashed lines enclose the area representing the mean $\pm 1\sigma$ calculated for the remaining samples. Note the scale changes at 4000 and 500 years. Abbreviations for eruptive periods are AC, Ape Canyon; CO, Cougar; SW, Swift Creek; SM, Smith Creek; PI, Pine Creek; CC, Castle Creek; SB, Sugar Bowl; K, Kalama; GR, Goat Rocks; and P, present.

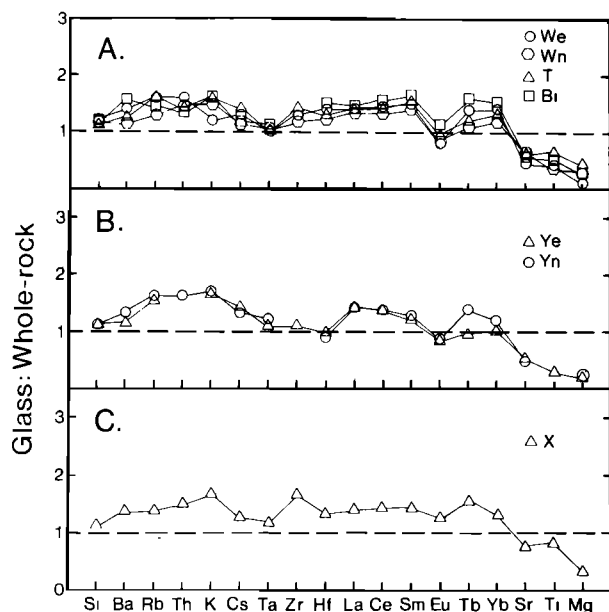


Fig. 7. Matrix glass compositions normalized to whole-rock compositions for selected Mount St. Helens pumices and scoria. (a) Glass:whole - rock ratios for dacites that do not include cummingtonite in the phenocryst assemblage (We, Wn, T, Bi). (b) Glass:whole - rock ratios for dacites that contain cummingtonite phenocrysts (Ye and Yn). (c) Glass:whole-rock ratios for an andesitic scoria (X).

Crystal Fractionation

Simple crystal fractionation models can be tested using (1) empirical enrichment/depletion patterns (e.g., Figure 7) for assumed daughter-parent liquid pairs and (2) calculated apparent bulk distribution coefficients (Table 7). It is assumed for the present that whole - rock dacite analyses indeed approximate magmatic compositions.

The patterns for Sugar Bowl rhyodacites normalized to several lesser evolved dacites (Figure 8b) are similar to glass/whole - rock patterns and thus suggest that the compositional variation among dacite magmas could result from crystal fractionation processes (*sensu lato*). However, the Sugar Bowl/East dome dacites have slightly higher $^{87}\text{Sr}/^{86}\text{Sr}$ ratios than other dacites [Smith et al., 1983; Halliday et al., 1983], so additional factors (slight crustal contamination or source variability) are required to satisfy all data.

Normalized patterns for coeval dacite:andesite pairs from the Kalama and Goat Rocks periods (Figure 9) and for representative dacite:basalt pairs (Figure 10) argue strongly against derivation of the dacites from any of these more mafic magmas by crystal fractionation processes. In most cases, incompatible elements to the right of Cs (i.e., Nb to Sm) are actually depleted in the dacites, and in many cases, Ba, Rb, Th, K, and Cs exhibit variable enrichments that are inconsistent with the generally uniform and low bulk distribution coefficients expected for these elements (notwithstanding possible volatile transfer losses). In Figure 10a, normalized values for Sr are also greater than unity, which seems inconsistent with closed - system fractionation given the

TABLE 7. Apparent Bulk Distribution Coefficients

	Unit							Mean*
	T	Bi	We	Wn	Ye	Yn	X	
F	0.60	0.59	0.50	0.63	(0.55)†	0.55	0.54	
Ba	0.59	0.18	0.50	0.68	0.74	0.53	0.49	0.54 (0.18)
Rb	0.06	0.31	0.34	0.43	0.25	0.19	0.46	0.26 (0.12)
Th	0.31	0.43	0.31	0.21	0.19	(0.80)‡	0.31	0.29 (0.09)
K	0.11	0.14	0.38	0.16	0.13	0.11	0.16	0.17 (0.09)
Cs	0.35	0.63	0.62	0.71	0.40	0.49	0.58	0.53 (0.13)
Ta	0.91	0.79	0.97	1.00	0.85	0.66	0.69	0.86 (0.11)
Zr	0.33		0.60	0.61	0.81			0.59 (0.17)
Hf	0.47	0.25	0.51	0.50	1.00	1.12	0.51	0.43 (0.11)
								1.06 (0.06)§
La	0.34	0.31	0.50	0.33	0.36	0.36	0.47	0.37 (0.06)
Ce	0.31	0.18	0.48	0.35	0.45		0.40	0.35 (0.11)
Sm	0.17	(0.04)‡	0.40	0.24	0.45	0.57	0.38	0.37 (0.14)
Eu	1.09	0.77	1.30	1.27	1.25	1.22	0.57	1.15 (0.18)
Tb	0.61	0.11	0.53	0.79	(1.05)‡	0.43	0.25	0.49 (0.23)
Yb	0.43	0.17	0.52	0.58	0.92	0.65	0.55	0.55 (0.23)
Sr	1.95	2.16	2.20	1.93	1.98	2.09	1.32	2.05 (0.10)

Apparent bulk distribution coefficients (D) were calculated for selected samples using trace element data for glass:whole - rock pairs and Shaw's [1970] equation for Rayleigh fractionation. Because most elements are largely incompatible, the calculated D's are not significantly changed if Nernst fractionation is assumed. The amount of matrix glass in the whole rock samples (Table 2) was taken to represent F, and the concentration of the element in the glass and whole - rock represented C_1 and C_0 , respectively.

* Mean bulk distribution coefficient (D) and standard deviation calculated from D's for the dacite pumices; andesitic scoria X was excluded.

† Estimated, as major element mixing models gave high residual sums or unreasonable mineral proportions.

‡ Not included in mean (last column).

§ First mean is for samples that do not contain cummingtonite (T, Bi, We, and Wn), and second mean is for samples that contain cummingtonite (Ye and Yn).

abundance of plagioclase in all Mount St. Helens eruptive products [Smith, 1984] and resulting high bulk D values indicated for Sr in such assemblages. Thus we conclude that the dacite liquids commonly are more depleted in most incompatible elements (except the hygromagmatic elements) than any reasonable mafic parental liquids.

This point is further emphasized by comparison with trace element enrichment patterns for silicic lavas from Medicine Lake where it is proposed that dacites and rhyolites are derived from andesitic parental magmas primarily via crystal fractionation [Grove and Donnelly-Nolan, 1986]. Unlike the case for Mount St.

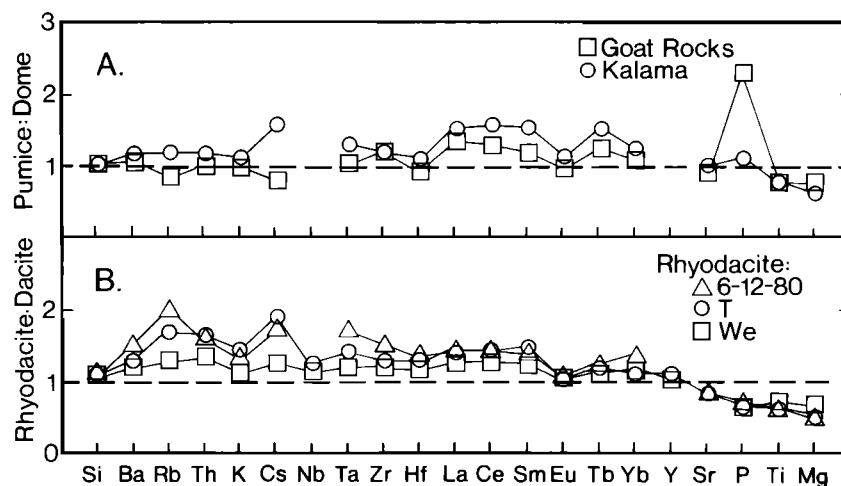


Fig. 8. (a) Dacite pumices (T and We) normalized to coeval dacite domes (Goat Rocks and Summit) of the Goat Rocks and Kalama eruptive periods. (b) Average Sugar Bowl rhyodacite normalized to selected dacites.

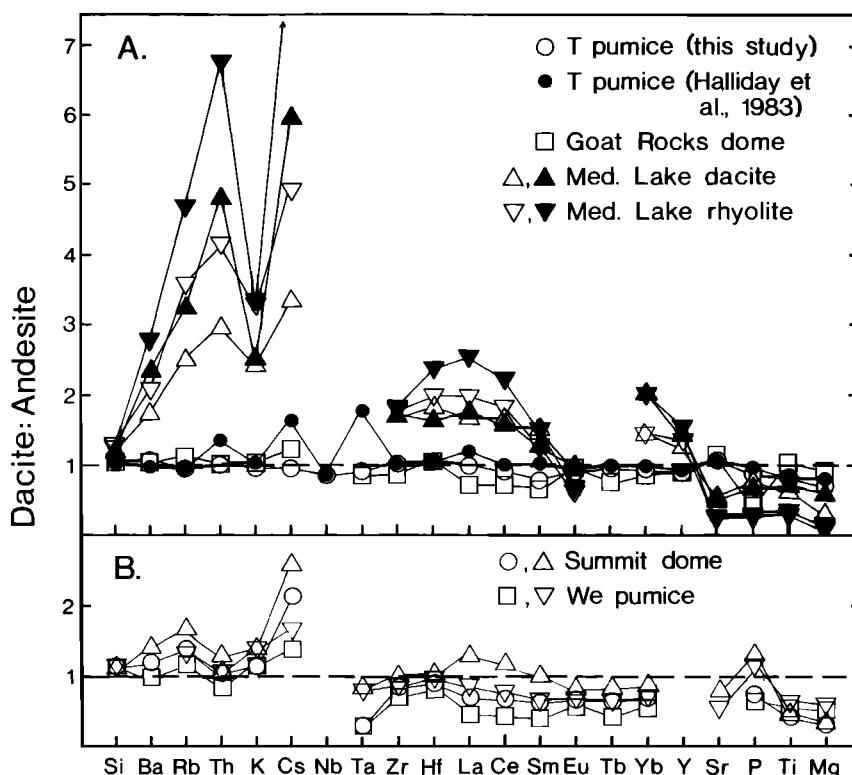


Fig. 9. (a) Goat Rocks period T pumice and Goat Rocks dome normalized to Goat Rocks period andesite lava. Also shown are Medicine Lake dacite (403Mg) and rhyolite (404M) normalized to Medicine Lake andesitic inclusions (an average of samples 278M and 403Me [Grove and Donnelly-Nolan, 1986]; open symbols) and Mount St. Helens Goat Rocks period andesite (solid symbols). (b) Kalama period We pumice and Summit dome normalized to coeval andesite lavas.

Helens dacites, those from Medicine Lake exhibit marked incompatible element enrichments when normalized to compositions of associated andesites (Figure 9a).

Because the above conclusion depends on our assumption that the dacites represent magmatic compositions, it is of interest to evaluate this possibility. First, although the dacites typically are strongly porphyritic (~25 to 50% crystals), the phenocrysts tend to be quite small (generally 0.5 - 1 mm), and crystal clots (which might promote gravitational settling) are common only in dacitic domes and flows. It is unlikely that these crystals could have been efficiently removed from viscous dacite liquids by crystal settling. If crystal fractionation occurred by a process such as sidewall crystallization, then parental liquids must have been depleted in the incompatible elements relative to the analyzed dacites. Although accumulation of phenocrysts might dilute abundances of incompatible elements (with the possible exception of Sr), textural evidence suggests that the majority of phenocrysts grew in situ. Also, on an anhydrous basis, compositions of glasses included in phenocrysts and in pumice matrices are similar [cf. Melson, 1983; Rutherford et al., 1985]. Thus, these phases essentially were in compositional equilibrium and simple concentration of phenocrysts (e.g., via filter pressing) cannot account for the enrichment factors seen in the glass/whole-rock plots (Figure 7).

Because the effectiveness of crystal fractionation processes depends on magnitudes of bulk distribution coefficients, it is important to consider factors that might influence the D values. If D values lower than those estimated in Table 7 pertain, as in crystallization of mafic to intermediate parental magmas, then more extreme incompatible element enrichments should have resulted. If so, the parental liquid(s) must have been

more depleted in incompatible elements than the analyzed dacites and our conclusion is not modified.

Inclusion of accessory phases in the fractionating mineral assemblage could result in depletion (or limited enrichment) of elements strongly included in such phases [e.g., Hanson, 1980]. Because most of the nominally incompatible elements (except Ba, Rb, Th, K, Cs) display little if any enrichment in Mount St. Helens dacites (relative to more mafic parental liquids), one must postulate the simultaneous removal of several accessory phases to achieve this effect. In any case, suitable accessory phases (e.g., apatite, zircon, allanite, monazite) either were not observed in the dacites, or occur in such low abundance that they could not significantly buffer incompatible element concentrations. Furthermore, we know of no likely phases that could effectively extract Be and U, both of which have comparable abundances in Mount St. Helens dacite and basaltic lavas [Smith and Leeman, 1985].

In summary, based on trace element contents, it is difficult to call solely upon closed-system crystal fractionation of andesitic or basaltic magmas to generate dacites at Mount St. Helens. This conclusion is also supported by isotopic data. The dacites have higher $^{87}\text{Sr}/^{86}\text{Sr}$ (0.70351 - 0.70397) and ^{18}O (+6.7 to 7.4) and lower $^{143}\text{Nd}/^{144}\text{Nd}$ (0.512872 - 0.512994) ratios relative to Mount St. Helens basalts ($^{87}\text{Sr}/^{86}\text{Sr}$ = 0.70301 - 0.70313; ^{18}O = +5.7 to 5.9; $^{143}\text{Nd}/^{144}\text{Nd}$ = 0.512997 - 0.513035) [Smith et al., 1983; Smith and Leeman, 1985; Halliday et al., 1983].

Magma Mixing/Assimilation Processes

Elevated strontium and oxygen ratios and lower neodymium ratios relative to presumably mantle-derived

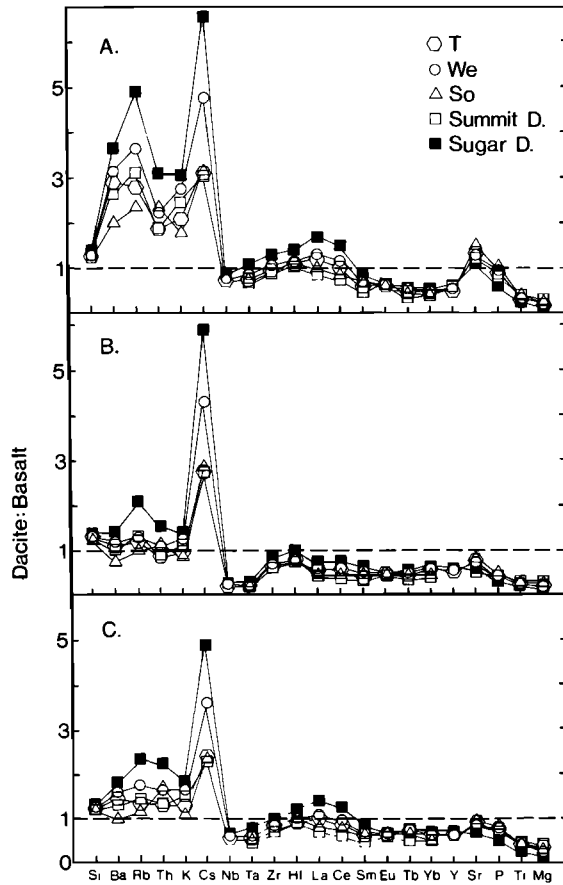


Fig. 10. Selected Mount St. Helens dacites normalized to mafic lavas erupted at Mount St. Helens during the Castle Creek eruptive period. Dacites are normalized to (a) average tholeiitic basalt (the Cave basalt), (b) average calcalkaline basalt, and (c) average basaltic andesite.

basaltic magmas suggest that dacite petrogenesis involved a crustal (or at least a relatively enriched) component. For example, the dacites may have been produced by mixing of mantle - derived basaltic magmas with crustal - derived silicic magmas, or by assimilation combined with fractional crystallization processes.

The presence of disequilibrium mineral assemblages and zoning patterns have been used as evidence that magma mixing is an important process at some volcanic centers [e.g., Sakuyama, 1979; Eichelberger and Gooley, 1977]. Reverse zoning in some ferromagnesian and plagioclase phenocrysts, resorbed plagioclase cores, and the presence of refractory olivine and clinopyroxene in some of the dacites suggest that magma mixing may have operated at Mount St. Helens (e.g., Goat Rocks and Kalama period eruptive products). Based on petrographic and geochemical data, Pallister and Hoblitt [1985] came to the same conclusion. The wide range in several incompatible element ratios in dacites of the Kalama eruptive period is also consistent with magma mixing. However, because the dacites have contents of many incompatible elements similar to or lower than those in Mount St. Helens andesitic and basaltic magmas (Figures 9 and 10), the postulated felsic mixing endmember magma(s) could not have been enriched in those elements compared with the mafic magma. Similarly, an origin of

the dacites due to assimilation of a crustal component by mafic magmas requires that the crustal component be compositionally similar to or more depleted than the basaltic magmas. Thus, the origin of incompatible element - poor silicic magmas is a fundamental petrologic problem at Mount St. Helens. The remainder of this paper focuses on attempts to model the felsic endmember magmas (and perhaps the dacites themselves) essentially via partial melting processes.

Partial Melting

Wyllie [1984] recently reviewed possible sites of magma generation at convergent ocean/continent plate boundaries. Likely melting sites include (1) the subducted oceanic crust, (2) the overlying mantle wedge, and (3) the lower continental crust. Although some mafic magmas may be produced in the mantle wedge, it is improbable that dacitic or even andesitic magmas are produced by direct partial fusion of peridotite in this environment even if the wedge was "contaminated" by slab - derived fluids and melts [Wyllie, 1979, 1982]. Silicic magmas may be generated by partial melting of subducted oceanic crust, or the lower crust in mature island arcs or continental arcs [Green, 1980; Wyllie, 1984]. Subducted oceanic crust may comprise fresh and/or altered midocean ridge basalts and gabbros, and perhaps a veneer of oceanic sediments, all of which would be subjected to metamorphism with progressive burial. There is wider latitude in selecting continental crustal compositions, but in the southern Washington Cascades, the crust is relatively young and largely oceanic in character. Eocene and younger rocks exposed in the vicinity of Mount St. Helens include orogenic volcanic rocks, volcanoclastic sediments, and continental margin detrital sediments resting on a mafic oceanic crust. Crustal xenoliths in 1980 - 1983 Mount St. Helens eruptive products include gabbros, hornfelsed basaltic lavas, amphibolites, hornblendites, diabase, and vein quartz [Moore et al., 1981; Heliker, 1983].

Dacitic to rhyolitic melts similar to those from Mount St. Helens have been produced experimentally by partial melting of hydrous basaltic rocks over a range in temperature (~700 to 1000°C) and oxygen fugacity (quartz - fayalite - magnetite to the hematite - magnetite buffers) [e.g., Holloway and Burnham, 1972; Helz, 1976]. Intensive parameters for Mount St. Helens dacite magmas estimated from compositions of coexisting ilmenite and magnetite (Table 5) resemble those in Helz's experiments, in which melt compositions varied with temperature and degree of melting. Mount St. Helens dacites and the melts produced in Helz's experiments are similar in composition, except for FeO and MgO, which are higher in the natural dacites (Figure 11).

Given this similarity, we modeled trace element compositions of hypothetical basaltic source rocks that upon partial melting could produce typical Mount St. Helens dacite magma (Figure 12). Based on the experimental results of Holloway and Burnham [1972] and Helz [1976], it was assumed that only amphibole, clinopyroxene, and plagioclase were involved in melting; melting and modal proportions in the hypothetical source rocks were estimated from the experimental results. Relative concentrations (C_1/C_0) of trace elements between the melt (C_1) and source (C_0) were calculated for equilibrium and fractional melting models at degrees of melting (30-50%) consistent with Helz's experiments. The measured trace element contents in average Mount St. Helens dacite (C_1) were then used to calculate the source

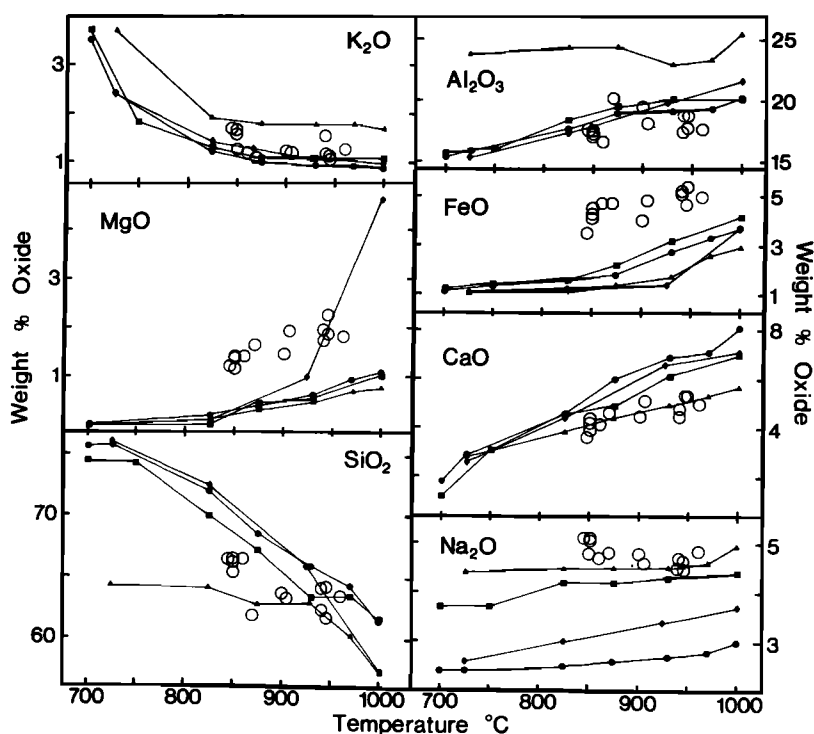


Fig. 11. Major element compositions of selected Mount St. Helens dacites (open circles) plotted versus temperature estimated by the method of Spencer and Lindsley [1982] (see Table 5 of this study). Temperatures estimated by the method of Andersen and Lindsley [1985] shift the points to temperatures (on the average) -35°C lower than those shown. Also shown are compositions of partial melts in various starting compositions from Helz's [1976, Figure 2] experiments.

TABLE 8. Trace Element Compositions of Typical MORB and Selected Sediments

	Sample				
	MORB*	Tyee1†	Tyee2†	487CS‡	19W‡
Ba	11	825	921	6875	703
Rb	2	124	75	51	186
Th	0.45	11.50	10.10	4.06	16.80
Cs	0.02	8.39	2.32		
Nb	3.5	18.0	14.0	5.1	10.9
Ta	0.18	1.20	0.95	0.32	1.78
Zr	90	164	181	124	189
Hf	2.4	4.4	4.8	2.6	5.1
La	3.9	34.4	31.7	76.0	24.0
Ce	10.8	69.5	62.2	50.0	63.0
Sm	3.22	6.03	5.17	12.05	3.75
Eu	1.13	1.32	1.26	3.13	0.80
Tb	0.74	0.83	0.59		
Yb	3.12	2.24	1.77	7.47	2.97
Sr	105	279	493	319	85
Ni	110	47	18	324	45
V	260	131	82		

* See appendix for data sources.

† Tyee sediments analyzed by N. Rogers (INAA, Open University) and W. Leeman (XRF, Open University).

‡ From Thompson et al. [1984, appendix A1].

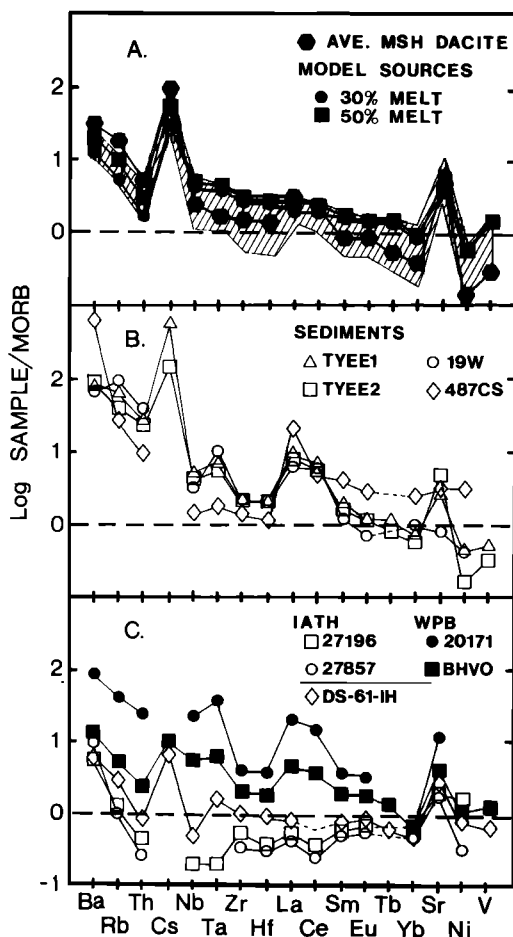


Fig. 12. MORB - normalized trace element patterns for (a) Mount St. Helens average dacite used to calculate source models, a representative calculated source composition involving 30% and 50% melting, and the range of calculated source compositions for various models involving different source and melting modes (diagonally ruled; see appendix for details of model parameters). (b) Marine sediments (Tyee1 and Tyee2, (this study) and 487CS and 19W [Thompson et al., 1984]). (c) Representative island arc tholeiites (IATH) (Thompson et al. [1984], samples 27196 and 27857) and within-plate basalts (WPB) (Thompson et al. [1984], 20171; Govindaraju, [1984], BHVO). Also shown is Cascade Quaternary tholeiitic basalt (Smith [1984], DS-61-IH).

rock trace element abundances (C_0). A compilation of model parameters used is given in the appendix.

Figure 12a illustrates average Mount St. Helens dacite melt and calculated source compositions normalized to a typical midocean ridge basalt (MORB). For some models, the estimated sources have fairly flat MORB - normalized patterns, except for notable enrichments in Ba, Rb, Cs, and Sr. However, if the dacite-parental magmas were more depleted than the average dacite (i.e., enrichment of incompatible elements in the erupted dacites resulted from such processes as fractionation, magma mixing, or assimilation), then the calculated sources must be even more depleted than illustrated. Other model sources exhibit slight enrichments in LREE and depletions in HREE relative to MORB, but typically lack enrichment in Nb and Ta (Figure 12).

Calculated enrichments for hygromagmatic elements must represent lower limits if the dacite liquids lost some of these elements via volatile transfer processes. In any case, source enrichments for these elements could reflect addition of a sedimentary component [Kay, 1984]. To test this possibility, we analyzed two Eocene Tyee sediments (a shale and a graywacke) that could represent crustal lithologies or subducted sedimentary material. Our data and selected published analyses for oceanic sediments are given in Table 8 and are shown normalized to MORB in Figure 12b. The shapes of the normalized sediment patterns resemble the estimated dacite source patterns, especially in the marked enrichments in Ba, Rb, Cs, and Sr (and LREE). It appears that mixtures of MORB-like mafic material with such sediments could approximate the incompatible trace element characteristics of our calculated sources, but in detail, simple mixtures of these components fail to provide a quantitative match. Considering the Tyee sediments as possible ingredients, some elements (e.g., Sr) require very large proportions of sediment, whereas others (e.g., Ba and Rb) require much less sediment.

Because volcanic arc basalts are commonly enriched in the hygromagmatic elements, it has been proposed that (1) these elements may be mobilized in aqueous fluids extracted during dehydration of the subducted slab and (2) movement of such fluids could produce selective and localized enrichments of hygromagmatic element contents (e.g., in the overlying mantle or crust) [cf. Pearce, 1983; Hole et al., 1984]. In the case of dacite magma genesis, the source(s) could be mafic rocks that have been metasomatically enriched by interaction with such fluids. It is possible that such source rocks could reside in the subducted slab itself (i.e., oceanic crust comprising basalts and sediments), or in the continental crust, where metasomatizing fluids and heat could be related to intrusions of large mafic magma bodies.

Available isotopic data [Church and Tilton, 1973; Church, 1976; Halliday et al., 1983; Smith et al., 1983; Smith and Leeman, 1985] indicate that the dacites contain a significant crustal component, and Church [1976] has proposed that they are melts of a mixture of crustal igneous rocks and sediments. Our results are in accord with such a model, but the isotopic data alone do not exclude altered subducted slab as a magma source. However, metamorphism of the slab to eclogite facies with progressive burial would produce a source (garnet-bearing) that would strongly buffer HREE contents and produce melts with high La/Yb ratios. Because Mount St. Helens dacites are depleted in Zr as well as HREE relative to associated basalts, Halliday et al. [1983] argued that zircon, rather than garnet, was an important buffering phase. They also proposed that Pb isotopic compositions and Yb and Zr contents are indicative of contributions of old crustal zircons to the dacitic magmas. However, the low abundance of zircon (and Zr) in Mount St. Helens dacites (trace zircon was observed in only one sample) is inconsistent with models involving zircon addition or fractionation to explain the wide variations in Zr and Yb contents the Mount St. Helens lavas. We suggest that these characteristics may be attributed to partial melting of an amphibole-rich metabasalt source in which bulk D values are large for both Yb and Zr [Pearce and Norry, 1979].

Conclusions

Our study presents new geochemical and petrologic information for dacitic rocks erupted throughout the evolution of Mount St. Helens. These results provide

TABLE A1. Mineral-Liquid Distribution Coefficients

	Amphibole	Plagioclase	Clinopyroxene	Fe-Ti Oxides	Apatite
Ba	0.10	0.36	0.3	0.001	0.01
Rb	0.05	0.05	0.1	0.001	0.01
Th	0.05	0.05	0.1	0.001	0.01
Cs	0.05	0.05	0.1	0.001	0.01
Nb	4.0	0.06	0.8	2.5	0.1
Ta	4.0	0.06	0.8	2.5	0.1
Zr	4.0	0.1	0.6	0.8	0.1
Hf	4.0	0.1	0.6	0.8	0.1
La	0.5	0.285	0.26	0.03	15
Ce	0.9	0.183	0.36	0.03	16.6
Sm	3.99	0.10	0.95	0.03	20.7
Eu	3.44	0.38	0.68	0.03	14.5
Tb	5.80	0.07	1.2	0.05	18.5
Yb	4.90	0.05	1.3	0.10	9.4
Sr	0.3	2.8	0.3	0.001	0.01
Ni	8.3	0.04	4	20	0.01
V	10	0.05	5	32	0.01

useful constraints on the petrogenetic evolution of the volcano and on possible origins of the dacitic magmas in particular.

1. Although some incompatible trace element ratios in the dacite magmas are nearly uniform through time (e.g., Ba/La, Rb/Cs, Hf/Ta), others are significantly varied (Th/Cs, Ba/Cs) (Figure 6) and seemingly preclude the existence of a single uniform magma reservoir as proposed by Halliday et al. [1983]. Our conclusion is supported by radioisotope studies [Bennett et al., 1982] that suggest a maximum age of about 150 years for the magma batch associated with the current eruptive phase. Either open-system processes were involved, or heterogeneous source regions were melted to produce distinct batches of dacitic magma.

2. Compositions of whole-rock and glass separates from selected pumice clasts provide estimates of bulk distribution coefficients for the analyzed trace elements, and are consistent with operation of crystal-liquid fractionation on the scale of individual magma batches.

3. Compositional variations among dacites of some eruptive periods apparently result from effects of crystal fractionation, magma mixing, or assimilation. Sugar Bowl rhyodacites appear to be derived from a dacitic parent magma by combined assimilation and fractionation. Wide compositional variations and presence of disequilibrium phenocrysts in lavas of the Kalama and Goat Rocks eruptive periods indicate that mixing of mafic and silicic magmas played a role in their origin.

4. With regard to contents of most incompatible

TABLE A2. Melting and Source Modes Used in Partial Melting Calculations

Model	Amphibole	Plagioclase	Clinopyroxene	Oxides	Apatite
<u>Melting Modes</u>					
A	0.10	0.90			
B	0.55	0.45			
C	0.55	0.45			
D	0.10	0.90			
E		0.75	0.25		
H		0.75	0.25		
J		0.75	0.25		
<u>Source Modes</u>					
A	0.40	0.55		0.04	0.01
B	0.40	0.55		0.04	0.01
C	0.25	0.70		0.04	0.01
D	0.25	0.70		0.04	0.01
E		0.70	0.25	0.04	0.01
H		0.55	0.40	0.04	0.01
J	0.20	0.60	0.15	0.04	0.01

TABLE A3. Average Trace Element Abundances for Mount St. Helens Dacites and Midocean Ridge Basalt

	Average	MORB*
Cs	1.49	0.016
Th	2.42	0.45
Ba	350	11
Rb	34	2
Nb	8.0	3.5
Ta	0.44	0.18
Zr	132	90
Hf	3.2	2.4
La	11.6	3.9
Ce	24.3	10.8
Sm	2.53	3.22
Eu	0.87	1.13
Tb	0.38	0.74
Yb	1.20	3.12
Sr	470	105
Ni	15	110
V	71	260

* Cs, Ba, and Rb from Sinha and Hart [1972]. Ta, Nb, Zr, and Hf from Pearce [1982, p. 527]. V is an average value from Sun et al. [1979]. Values for the remaining elements are the averages of samples OF-4, OF-11, OF-15, and OF-16 in the Basaltic Volcanism Study Project [1981, Table 2, microfiche appendix, section A-5].

elements, the dacites are similar in composition to associated basaltic and andesitic lavas. This surprising observation precludes derivation of the dacites from any of the more mafic erupted magmas by crystal fractionation processes.

5. It is more plausible that the dacitic magmas formed by large degrees of partial melting of an amphibolite facies crustal source characterized by MORB-like relative abundances of most incompatible trace elements, with exception of the hygromagmatic elements (Ba, Rb, K, Cs, and Sr) which are relatively enriched in the source. This combination of compositional characteristics (i.e., decoupling of incompatible element behavior) is consistent with involvement of one or more of the following source components: (a) relatively primitive island arc tholeiites (or altered MORB?) that are already enriched in hygromagmatic elements (cf. Pearce, 1983); (b) sedimentary rocks or sediments similar to the analyzed Tyee samples (cf. Hole et al., 1984; Kay, 1984); and (c) metasomatized rocks that interacted with fluids enriched in hygromagmatic elements.

Appendix: Partial Melting Models

Shaw's [1970] equations for equilibrium and fractional melting were used in partial melting calculations involving the generation of dacitic liquids from basaltic source rocks. Table A1 lists the mineral-liquid distribution coefficients (K_D 's) used in calculating C_1/C_0 ratios. K_D 's used are from Hanson [1980], Pearce and Norry [1979], appendix IV of Smith [1984], or are estimates.

Source and melting modes are given for representative models in Table A2. Other models included apatite and/or oxides in the source, but at the high degrees of melting (30-50%) assumed, these gave essentially the same results

as shown in Figure 12a. The model calculations yield C_1/C_0 ratios (where C_1 is concentration of an element in the liquid and C_0 is concentration in the source rock) at various degrees of melting under equilibrium and fractional melting conditions. Dacite compositions were assumed to represent C_1 , thus the source rock compositions (C_0) were calculated for various models and normalized to MORB for purposes of comparison (cf. Figure 12). Table A3 gives trace element compositions for typical MORB used in normalizations, and the average dacite composition used to calculate source compositions. The dacite is an average of three units (Bi, T, and Py) that were selected because, among the dacites studied, their major element compositions and estimated temperatures are most similar to Helz's [1976] experimentally produced melts.

Acknowledgments. This research was supported by the National Science Foundation (grants EAR79-19998, EAR82-14876, and EAR85-12172). D.R.S. acknowledges additional summer support from Trinity University and the Penrose Foundation. We thank Roman Schmitt (Oregon State University) and Doug Blanchard (NASA-JSC) for access to neutron activation facilities and John Watson (Open University) for access to X-ray fluorescence facilities. We thank Don Mullineaux for introducing us to the stratigraphy at Mount St. Helens, Bill Melson for providing several key samples, Cliff Hopson for a copy of his geologic map of Mount St. Helens, and Zell Peterman for providing samples of Tyee sediments. Special thanks go to Marc Norman and Godfrey Fitton for providing analyses of the L82 samples, and to Randy Hermens for field assistance. Critical reviews by David Gerlach, Howard West, Robert Freed, and two anonymous reviewers greatly contributed to the quality of the manuscript.

References

- Andersen, D. J. and D. H. Lindsley, New (and final) models for the Ti-magnetite/ilmenite geothermometer and oxygen barometer, *Eos Trans. AGU*, **66**, 416, 1985.
- Arth, J. G. and Barker, F., Rare-earth partitioning between hornblende and dacitic liquid and implications for the genesis of trondjhemitic-tonalitic magmas, *Geology*, **4**, 534-536, 1976.
- Basaltic Volcanism Study Project, *Basaltic Volcanism on the Terrestrial Planets*, 1286 pp., Pergamon, New York, 1981.
- Bennett, J. T., S. Krishnaswami, K. K. Turekian, W. G. Melson, and C. A. Hopson, The uranium and thorium decay series nuclides in Mt. St. Helens effusives, *Earth Planet. Sci. Lett.*, **60**, 61-69, 1982.
- Berman, R. G., Differentiation of calc-alkaline magmas: Evidence from the Coquihalla volcanic complex, British Columbia, *J. Volcanol. and Geotherm. Res.*, **9**, 151-179, 1981.
- Cashman, K. V. and J. E. Taggart, Petrologic monitoring of 1981 and 1982 eruptive products from Mount St. Helens, *Science*, **221**, 1385-1387, 1983.
- Church, S. E., The Cascade Mountains revisited: A re-evaluation in the light of new lead isotopic data, *Earth Planet. Sci. Lett.*, **2**, 175-188, 1976.
- Church, S. E. and G. R. Tilton, Lead and strontium isotopic studies in the Cascade Mountains: Bearing on andesite genesis, *Geol. Soc. Am. Bull.*, **84**, 431-454, 1973.
- Crandell, D. R. and D. R. Mullineaux, Pine Creek assemblage at Mount St. Helens, Washington, *U.S. Geol. Surv. Bull.*, **1383-A**, 23 pp., 1973.
- Crandell, D. R. and D. R. Mullineaux, Potential hazards

- from future eruptions of Mount St. Helens volcano, Washington, U.S. Geol. Surv. Bull., **1383-C**, 16 pp., 1978.
- Crandell, D. R., D. R. Mullineaux, and M. Rubin, Mount St. Helens volcano: Recent and future behavior, Science, **187**, 438-441, 1975.
- Deruelle, B., R. S. Harmon, and S. Moorbath, Combined Sr-O isotope relationships and petrogenesis of Andean volcanics of South America, Nature, **302**, 814-816, 1983.
- Drake, M. J. and D. R. Weill, Partitioning of Sr, Ba, Ca, Y, Eu²⁺, Eu³⁺, and other REE between plagioclase feldspar and magmatic liquid: An experimental study, Geochim. Cosmochim. Acta, **39**, 689-712, 1975.
- Eichelberger, J. C., Origin and andesite and dacite: Evidence of mixing at Glass Mountain in California and other Circum-Pacific volcanoes, Bull. Geol. Soc. Am., **86**, 1381-1391, 1975.
- Eichelberger, J. C. and R. Gooley, Evolution of silicic magma chambers and their relationship to basaltic volcanism, Geophys. Monogr. Am. Geophys. Union, **20**, 57-77, 1977.
- Garcia, M. O., and S. S. Jacobson, Crystal clots, amphibole fractionation and the evolution of calc-alkaline magmas, Contrib. Mineral. Petrol., **69**, 319-327, 1979.
- Gerlach, D. C. and T. L. Grove, Petrology of Medicine Lake Highland volcanics: Characterization of end-members of magma mixing, Contrib. Mineral. Petrol., **80**, 147-159, 1982.
- Gill, J. B., Orogenic Andesites and Plate Tectonics, 390 pp., Springer-Verlag, New York, 1981.
- Govindaraju, K., 1984, Compilation of working values and sample description for 170 international reference samples of mainly silicate rocks and minerals, Geo-standards Newsl., **8**, 1984.
- Grant, N. K., W. I. Rose, Jr., and L. A. Fultz, Correlated Sr isotope and geochemical variations in basalts and basaltic andesites from Guatemala, in Andean Magmatism: Chemical and Isotopic Constraints, edited by R. S. Harmon and B. A. Barreiro, pp. 139-149, Shiva Publishing, United Kingdom, 1984.
- Green, T. H., Island arc and continent-building magmatism--A review of petrogenetic models based on experimental petrology and geochemistry, Tectonophysics, **63**, 367-383, 1980.
- Grove, T. L., and J. M. Donnelly-Nolan, The evolution of young silicic lavas at Medicine Lake Volcano, California: Implications for the origin of compositional gaps in calc-alkaline series lavas, Contrib. Mineral. Petrol., **92**, 281-302, 1986.
- Halliday, A. N., A. E. Fallick, A. P. Dickin, A. B. MacKenzie, W. E. Stephens, and W. Hildreth, The isotopic and chemical evolution of Mount St. Helens, Earth Planet. Sci. Lett., **63**, 241-256, 1983.
- Hanson, G. N., Rare earth elements in petrogenetic studies of igneous systems, Annu. Rev. Earth Planet. Sci., **8**, 371-406, 1980.
- Harmon, R. S., R. S. Thorpe, and P. W. Francis, Petrogenesis of Andean andesites from combined Sr-O relationships, Nature, **290**, 396-399, 1981.
- Heliker, C. C., Inclusions in the 1980-1983 dacite of Mount St. Helens, Eos Trans. AGU, **64**, 894, 1983.
- Helz, R. T., Phase relations of basalts in their melting ranges at P_{H₂O} = 5 kb, II, Melt compositions, J. Petrol., **17**, 139-193, 1976.
- Hildreth, W., Gradients in silicic magma chambers: Implications for lithospheric magmatism, J. Geophys. Res., **86**, 10153-19182, 1981.
- Hoblitt, R. P., D. R. Crandell, and D. R. Mullineaux, Mount St. Helens eruptive behavior during the past 1500 yrs., Geology, **8**, 555-559, 1980.
- Hole, M. J., A. D. Saunders, G. F. Marriner, and J. Tarney, Subduction of pelagic sediments: Implications for the origin of Ce-anomalous basalts from the Mariana Islands, J. Geol. Soc. London, **14**, 453-472, 1984.
- Holloway, J. R. and C. W. Burnham, Melting relations of basalt with equilibrium water pressure less than total pressure, J. Petrol., **13**, 1-30, 1972.
- Hopson, C. A., Eruptive sequence at Mount St. Helens, Washington, Geol. Soc. Am. Abstr. Programs, **3**, 1381, 1971.
- Hopson, C. A., Origin of coherent and divergent lava suites at Quaternary andesitic volcanoes, Cascade Mountains, Geol. Soc. Am. Abstr. Programs, **4**, 172-173, 1972.
- Hyde, J. H., Upper Pleistocene pyroclastic-flow deposits and lahars south of Mount St. Helens volcano, Washington, U.S. Geol. Surv. Bull., **1383-B**, 20 pp., 1975.
- Kay, R. W., Elemental abundances relevant to identification of magma sources, Philos. Trans. R. Soc. London, Ser. A, **310**, 535-547, 1984.
- Lawrence, D. B., Continuing research on the flora of Mount St. Helens, Mazama, **21**, 45-54, 1939.
- Lawrence, D. B., Diagrammatic history of the northeast slope of Mount St. Helens, Washington, Mazama, **36**, 41-44, 1954.
- Lipman, P. W., D. R. Norton, J. E. Taggart, Jr., E. L. Brandt, and E. E. Engleman, Compositional variations in the 1980 magmatic deposits, U.S. Geol. Surv. Prof. Pap., **1250**, 631-640, 1981.
- Lopez-Escobar, L., Petrology and chemistry of volcanic rocks of the southern Andes, in Andean Magmatism: Chemical and Isotopic Constraints, edited by R. S. Harmon and B. A. Barreiro, pp. 47-71, Shiva Publishing, United Kingdom, 1984.
- Ludden, J. N. and G. Thompson, An evaluation of the behavior of the rare earth elements during the weathering of seafloor basalts, Earth Planet. Sci. Lett., **43**, 85-92, 1979.
- Mahood, G. A. and E. W. Hildreth, Large partition coefficients for trace elements in high silica rhyolites, Geochim. Cosmochim. Acta, **47**, 11-30, 1983.
- Matsuhisa, Y. and H. Kurassawa, Oxygen and strontium isotopic characteristics of calcalkalic volcanic rocks from the central and western Japan arcs: Evaluation of contribution of crustal components to the magmas, J. Volcanol. Geotherm. Res., **18**, 483-510, 1983.
- Melson, W. G., Monitoring the 1980-82 eruptions of Mount St. Helens: Compositions and abundances of glass, Science, **221**, 1387-1391, 1983.
- Melson, W. G. and C. A. Hopson, Preeruption temperatures and oxygen fugacities in the 1980 eruptive sequence, U.S. Geol. Surv. Prof. Pap., **1250**, 641-648, 1981.
- Merzbacher, C. L. and D. H. Egger, A magmatic geohygrometer: Application to Mount St. Helens and other dacitic magmas, Geology, **12**, 587-590, 1984.
- Moore, J. G., W.P. Lipman, D. A. Swanson, and T. R. Alpha, Growth of lava domes in the crater, June 1980-January 1981, U.S. Geol. Surv. Prof. Pap., **1250**, 541-547, 1981.
- Mullineaux, D. R., Summary of pre-1980 tephra-fall deposits erupted from Mount St. Helens, Washington state, USA, Bull. Volcanol., **1**, 17-26, 1986.
- Mullineaux, D. R. and D. R. Crandell, The eruptive history of Mount St. Helens, U.S. Geol. Surv. Prof. Pap., **1250**, 3-15, 1981.
- Mullineaux, D. R., J. H. Hyde, and M. Rubin, Widespread late glacial and postglacial tephra deposits from Mount St. Helens volcano, Washington, U.S. Geol. Surv. J. Res., **3**, 239-335, 1975.
- Nash, W. P. and H. R. Crecraft, Partition coefficients for

- trace elements in silicic magmas, Geochim. Cosmochim. Acta, **49**, 2309-2322, 1985.
- Pallister, J. R. and R. P. Hoblitt, Magma mixing at Mount St. Helens, Eos Trans. AGU, **66**, 1111, 1985.
- Pearce, J. A., Trace element characteristics of lavas from destructive plate boundaries, in Andesites: Orogenic Andesites and Related Rocks, edited by R. S. Thorpe, pp. 525-548, John Wiley, New York, 1982.
- Pearce, J. A., Role of sub-continental lithosphere in magma genesis at active continental margins, in Continental Basalts and Mantle Xenoliths, edited by M. J. Norry, pp. 230-249, Shiva Publishing, United Kingdom, 1983.
- Pearce, J. A. and M. J. Norry, Petrogenetic implications of Ti, Zr, Y, and Nb variations in volcanic rocks, Contrib. Mineral. Petrol., **62**, 33-47, 1979.
- Philpotts, J. A. and C. C. Schnetzler, Phenocryst-Matrix partition coefficients for K, Rb, Sr, and Ba with applications to anorthosite and basalt genesis, Geochim. Cosmochim. Acta, **34**, 307-322, 1970.
- Reid, F. W. and J. W. Cole, Origin of dacites of the Taupo volcanic zone, New Zealand, J. Volcanol. Geotherm. Res., **18**, 191-214, 1983.
- Rose, W. I., N. K. Grant, and J. Easter, Geochemistry of the Los Chocoyos ash, Quezaltenango valley, Guatemala, Geol. Soc. Am. Spec. Pap., **180**, 87-99, 1979.
- Rowley, P. D., M. A. Kuntz, and N. S. Macleod, Pyroclastic-flow deposits, U.S. Geol. Surv. Prof. Pap., **1250**, 489-512, 1981.
- Rutherford, M. J., H. Sigurdsson, S. Carey, and A. Davis, The May 18, 1980, eruption of Mount St. Helens, 1, Melt composition and experimental phase equilibria, J. Geophys. Res., **90**, 2929-2947, 1985.
- Sakuyama, M., Evidence for magma mixing: Petrological study of Shirouma-Oike calcalkaline andesite volcano, Japan, J. Volcanol. Geotherm. Res., **5**, 179-208, 1979.
- Scandone, R. and S. D. Malone, Magma supply, magma discharge and readjustment of the feeding system of Mount St. Helens during 1980, J. Volcanol. Geotherm. Res., **23**, 239-262, 1985.
- Scheidegger, K. F., A. N. Federman, and A. M. Tallman, Compositional heterogeneity of tephra from the 1980 eruptions of Mount St. Helens, J. Geophys. Res., **87**, 10861-10881, 1982.
- Shaw, D. R., Trace element fractionation during anatexis, Geochim. Cosmochim. Acta, **34**, 237-243, 1970.
- Sinha, A. K. and S. R. Hart, A geochemical test of the subduction hypothesis for generation of island arc magmas, Carnegie Inst. Wash. Yearb., **71**, 309-312, 1972.
- Smith, D. R., The petrology and geochemistry of High Cascade volcanics in southern Washington: Mount St. Helens volcano and the Indian Heaven basalt field, Ph.D. dissertation, Rice Univ., Houston, Tex., 409 pp., 1984.
- Smith, D. R. and W. P. Leeman, Mineralogy and phase chemistry of Mount St. Helens tephra sets W and Y as keys to their identification, Quat. Res., **17**, 211-227, 1982.
- Smith, D. R. and W. P. Leeman, Evidence against crystal fractionation in the generation of Mount St. Helens dacites, Eos Trans. AGU, **66**, 399, 1985.
- Smith, D. R., Y. Matsuhisa, H. Kurasawa, and W. P. Leeman, Oxygen and strontium isotopic variations in Mount St. Helens eruptive products, Eos Trans. AGU, **64**, 894, 1983.
- Smith, R. L., Ash-flow magmatism, Geol. Soc. Am. Spec. Pap., **180**, 5-27, 1979.
- Spencer, K. J. and D. H. Lindsley, A solution model for coexisting iron-titanium oxides, Am. Mineral., **66**, 1189-1201, 1982.
- Stormer, J. C., Jr., The effects of recalculation on estimates of temperature and oxygen fugacity from analyses of multicomponent iron-titanium oxides, Am. Mineral., **68**, 586-594, 1983.
- Sun, C. O., R. J. Williams, and S.-S. Sun, Distribution coefficients of Eu and Sr for plagioclase - liquid and clinopyroxene - liquid in oceanic ridge basalt: An experimental study, Geochim. Cosmochim. Acta, **38**, 1415-1433, 1974.
- Sun, S.-S., R. W. Nesbitt, and A. Y. Sharaskin, Geochemical characteristics of mid-ocean ridge basalts, Earth Planet. Sci. Lett., **44**, 119-138, 1979.
- Thompson, R. N., M. A. Morrison, G. L. Hendry, and S. J. Parry, An assessment of the relative roles of crust and mantle in magma genesis: An elemental approach, Philos. Trans. R. Soc. London, Ser. A, **310**, 549-590, 1984.
- Verhoogen, J., Mount St. Helens, A recent Cascade volcano, Calif. Univ. Dep. Geol. Sci. Bull., **24**, 263-302, 1973.
- Wyllie, P. J., Magmas and volatile contents, Am. Mineral., **64**, 41-71, 1979.
- Wyllie, P. J., Subduction products according to experimental prediction, Bull. Geol. Soc. Am., **93**, 468-476, 1982.
- Wyllie, P. J., Sources of granitoid magmas at convergent plate boundaries, Phys. Earth Planet. Inter., **35**, 12-18, 1984.

W. P. Leeman, Department of Geology and Geophysics, Rice University, Houston, TX 77251.

D. R. Smith, Geology Department, Trinity University, 715 Stadium Drive, San Antonio, TX 78284

(Received January 27, 1986;
revised August 28, 1986
accepted October 17, 1986.)